Non-invasive Detection of Cortical Control Signals for Brain-Computer Interfaces

Melissa M. Smith

A dissertation

submitted in partial fulfillment of the

requirements for the degree of

Doctor of Philosophy

University of Washington

2016

Reading Committee:

Rajesh Rao, Chair

Jeff Ojemann

Chet Moritz

Program Authorized to Offer Degree:

Graduate Program in Neuroscience

University of Washington

Abstract

Non-invasive Detection of Cortical Control Signals for Brain-Computer Interfaces

Melissa M. Smith

Chair of the Supervisory Committee:

Rajesh Rao, Professor
Computer Science and Engineering

In the sensorimotor areas of the cortex, motor execution and imagery have been found to be associated with increases in the high gamma (HG) frequency band, as well as decreases in the beta, and mu frequency bands. Because these cortical rhythms can be intentionally modulated by motor imagery or execution, they have often been used in brain-computer interface (BCI) studies as a control signal. However, the non-invasive recording of the modulation of the HG frequency band is still a relatively novel concept and most HG studies have been limited to invasive recording methods, due to the low signal-to-noise ratio of the neuronal ensemble activity at these frequencies. Consequently, the systematic study of HG effects has been limited to narrow populations (typically epilepsy patients) and cortical locations, which are usually determined by clinical needs rather than by the experimental paradigm one wishes to study. This thesis serves as a proof-of-concept that the HG frequency band can be studied non-invasively, thus opening up this band to a much wider subject population and range of experimental paradigms. In addition, this thesis provides evidence that an implanted subdermal recording electrode system may provide a reliable, long-term, portable method for recording these motor related control signals for BCI control.

TABLE OF CONTENTS

LIST OF FIGURES

LIST OF TABLES

ACKNOWLEDGEMENTS

I would like to give my sincerest gratitude for the mentoring and support of my mentor Rajesh Rao and dissertation committee members Jeff Ojemann, Chet Moritz, Tom Daniel, and Steve Perlmutter. I am so grateful that I had the privilege to learn from each of you. I would like to give a huge thanks to Felix Darvas for the enormous amount of guidance, patience, and mentoring he provided me during my dissertation. Thanks to Kurt Weaver for spending countless hours performing fMRI recordings with me. I would like to acknowledge the Grid lab and Neural Systems lab members for their support and numerous thoughtful discussions on MATLAB, signal processing, and neuroscience. Discussions I will greatly miss.

Thanks to the Center for Sensorimotor Neural Engineering for providing the financial support necessary to complete this dissertation.

Special thanks to my family for the love and support they provided me throughout my graduate education.

DEDICATION

For Shane and Aiken

Chapter 1. INTRODUCTION

A Brain-Computer Interface (BCI) is a system that acquires and analyzes brain signals with the goal of creating a communication channel between the brain and the computer (Wolpaw et al. 2002). BCIs have great potential to facilitate the lives of paralyzed individuals with intact brain function but damaged cortico-spinal pathways. Many non-invasive BCIs typically rely on slow cortical rhythms such as mu/alpha (8-12 Hz), beta (17-32 Hz), or evoked potentials (e.g. P300) for control signals. While these systems are working to a degree, overall efficacy is limited due to the time latency it takes, on the order of several hundred milliseconds, for the frequency band's amplitude to evolve (Pfurtscheller and Lopes da Silva 1999; Pfurtscheller and Lopes da Silva 1999). That is, the reliable detection of a response can take seconds for BCIs based on these control signals. This makes such systems unintuitive and cumbersome to use. Ideally, a smaller response lag is desired (i.e. 100 ms or less) to ensure a fluid, natural, and practical alternative to input devices that rely on motor movements such as keyboards, mice, eye trackers, etc. This requires cortical responses that can change rapidly within the desired lag time of the system.

The high gamma (HG) band has these properties; typical oscillations are greater than 70 Hz and detectable power shifts within this frequency band occur on very short time scales (~ 50 ms) (F Darvas et al. 2010). Another desirable property of the HG band is that it is spatially more focal than more slowly evolving potentials and thus highly specific to a given task (Kai J Miller et al. 2007). The HG band has been successfully used for BCI control using invasive electrocorticography (ECoG) techniques (Leuthardt et al. 2006). It has been shown that HG activity can be detected non-invasively by EEG in the primary motor area prior to finger movements (F Darvas et al. 2010). However, HG signals from surface EEG recordings suffer from two problems 1) low signal-to-noise ratio (SNR) and 2) overlap with EMG activity. In addition, due to the highly focal nature of the HG rhythm, single scalp electrodes, if not placed directly over the location of the source, can 'miss' power shifts in this frequency band.

However, due to the large range of potential changes for cortical point sources, the entire EEG montage can pick up these changes collectively, but with a very small signal in each electrode. The work described in chapters 2 and 3 of this thesis attempts to overcome these problems by using a combination of signal processing and cortical mapping techniques that utilize the subject's individual head anatomy acquired from MRI.

While we found that cortical neural signals can accurately be detected on the surface of the scalp through cortical mapping techniques, the neural signals detected with surface EEG electrodes still suffer from attenuation due to the fact that the signals need to pass through the thick skull and scalp. In addition, EEG electrodes are often contaminated with motion artifacts or changes in impedance values as the electrodes shift positions, or when the scalp muscles contract. Chapter 4 of this thesis presents results from needle electrode recordings that were placed underneath the scalp as an attempt to bypass these contaminations produced by movement and decrease portion of the signal attenuation due to the scalp. The results from the studies presented in this thesis may contribute to developing a rapid, long-term, EEG-based BCI that is capable of detecting motor signals so that control is approximately coincident with real-time intention.

The three main aims of this thesis are as follows and are discussed in chapters 2-4:

Aim 1. Detect high gamma non-invasively, using surface EEG electrodes, during imagined movement.

Significance: The first study to show that the high gamma frequency band can be detected non-invasively using surface EEG during a motor imagery task in healthy subjects using individual subject's head models.

Aim 2. Determine the degree of spatial correlation between the cortical representations of high gamma activity detected using surface EEG electrodes and BOLD fMRI signals generated from a motor imagery task.

Significance: The first study to examine the relationship between fMRI and the underlying neurophysiological responses during a motor imagery task.

Aim 3: Investigate the motor related brain activity of healthy subjects in the mu, beta, and high gamma frequency bands recorded using subdermal EEG electrodes.

Significance: Demonstrate a signal quality comparison of surface EEG and subdermal electrodes in awake/healthy subjects performing a motor execution task. These comparisons may support the use of subdermal recording electrodes as an option for long-term BCI use.

The following sections in this chapter will provide the basic neuroscience, BCI, and signal processing research background necessary to understand the intentions, methods, and results of the studies presented in Chapters 2-4.

1.1 CORTICAL NEURONAL ACTIVITY

Current BCI systems utilize the electric or magnetic signals produced by the nervous system to convey the user's intentions. In the brain, the electric fields are often described according to the location of the recording device and nature of the neural activity that produced the signal. The first category of electric fields includes local field potentials (LFPs). LFPs are recorded within the cortex and reflect current sources that are related to synaptic activity at a distance between 0.1-1.0 mm from the electrode. The second category includes the fields recorded on the surface of the cortex by ECoG electrodes, which are thought to reflect synaptic activity occurring at a depth of 2-5 mm below the surface of the cortex. The third category includes the electric fields recorded from the scalp using surface EEG electrodes. Each EEG electrode is thought to reflect

synaptic source activity that occurs over large portions of the underlying cortex (between 10-40 cm^2) and is thought to represent the average activity over a cortical region obtained from thousands of cortical neurons.

The work described in this thesis focuses on recording the electric fields recorded just below and above the scalp. It is thought that the EEG signal reflects the summation of excitatory and inhibitory postsynaptic potentials of populations of neurons with parallel orientations (Buzsáki, Anastassiou, and Koch 2012). These potentials are generated by the flow of ions into and out of the neuron. The orientation of the neurons producing the potentials within the cortex is one factor that determines how strong the signal will be at the scalp. Those neurons with radial orientation relative to the scalp will generate the strongest signals, while neurons with tangential orientations will likely cancel each other out and not contribute to the signal recorded at the scalp. The recorded electric field on the surface of the scalp is thought to be reflective of the synchronous neural activity of tens of thousands of cortical neurons (Murakami and Okada 2006).

An important consideration when recording neural signals from electrodes outside the brain is that the conductivity of the various intervening tissue layers (such as skull and scalp) between the brain and the electrode has a significant impact on the signal quality recorded at the electrode. The electric currents produced by neurons are strongly affected by jumps between these very conductive tissue layers. When trying to perform neuronal source localization the conductivity values of these tissue layers must be taken into consideration in order to produce accurate results. This subject is discussed a bit further in the section 1.6: *Cortical Source Localization.*

1.2 MOTOR ANATOMY AND NEUROPHYSIOLOGY

The vast majority of BCI research has focused on measuring brain signals thought to originate in the cortex because the cortex is accessible to electrodes and possesses defined areas known to be involved in motor and communication executive functions. These identifiable landmarks on the cortical surface in regions devoted to specific functions are often used to guide the placement of intracortical electrodes. In order for the signal features to be useful for controlling a BCI it is important that the user can modulate these recorded signals. A BCI user can volitionally modulate the oscillations in several frequency bands recorded in the sensorimotor regions and is one reason why BCIs are typically driven by cortical signals recorded over the motor cortex.

The following subsections will provide a brief background, along supporting published data, on the roles each cortical motor region (Figure 1.1) plays in the generation of movement. However, it must be kept in mind that research on the cortical role in movement is constantly evolving.

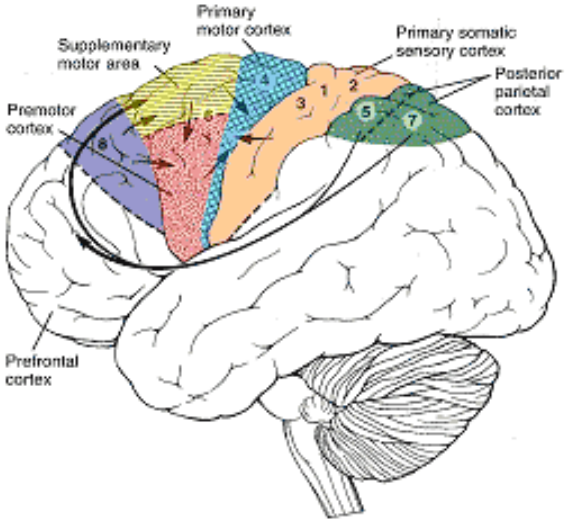

Figure 1.1. Motor areas of the cortex.

Adapted from: http://thebrainlabs.com

1.2.1 *Primary Motor Cortex*

The primary motor cortex (M1) is frequently used in BCI research because of its involvement in the execution and intention of movement. The M1 is located in the frontal lobe along the anterior wall of the central sulcus (caudal M1) and extends to the precentral gyrus (rostral M1). It is organized somatotopically such that certain regions of M1 are devoted to the control of particular parts of the body. This organization is depicted in Wilder Penfield's homunculus (Figure 1.2) (Penfield and Rasmussen 1950). The body parts shown in the homunculus are spatially distorted because the amount of cortical area devoted to control of certain body parts varies according to the complexity of the motor control of that body part.

Studies that support the notion that M1 is involved in motor execution show that the modulation of neural activity in M1 begins approximately 50-200ms before the onset of movement (a P. Georgopoulos et al. 1982). In addition, these studies showed evidence that M1 cortical neurons encode information about movement direction, a robust finding that has been replicated several times (Schwartz, Kettner, and Georgopoulos 1988; Kalaska, Caminiti, and Georgopoulos 1983). Additional kinematic features such as position, velocity, and movement distance have also been found to be encoded in M1. Other studies have shown that M1 activity is also modulated during movement intention and has been used to predict future movement directions (A. P. Georgopoulos 1989).

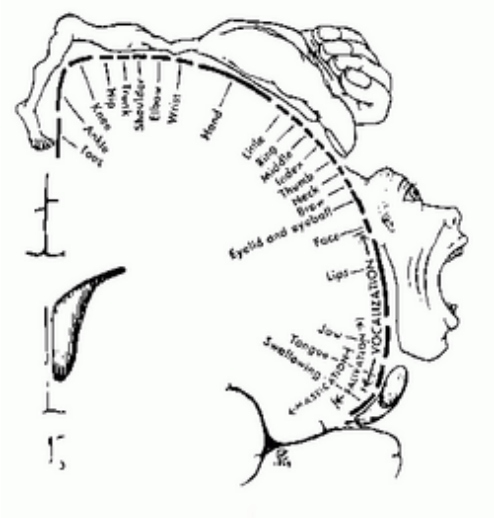

Figure 1.2. Motor Homunculus.

Adapted from Wilder Penfield, 1950

1.2.2 *Premotor Cortex*

The premotor cortex (PM) is located in the frontal lobe and is anterior to the primary motor cortex. Although electrical stimulations in the premotor cortices have been shown to also elicit movement similar to M1, the PM cortex is thought to be more involved in movement planning (Weinrich and Wise 1982; Crammond and Kalaska 2000; Hatsopoulos, Joshi, and O'Leary 2004). The PM cortex is divided into premotor dorsal (PMd) and ventral (PMv) areas, which are distinguished by their particular input originations and output destinations (Matelli et al. 1998; Ghosh and Gattera 1995). To complicate the PM cortex's role in movement, PMd neurons have been found to represent a target's location (Shen and Alexander 1997), while PMv neurons are thought to encode the direction of wrist-movement (Kakei, Hoffman, and Strick 2001). Medial to PMd is an area known as the supplementary motor area (SMA) that is located mostly within the interhemispheric fissure, but extends slightly onto exposed area of the cortex. This area is known to be involved with complex limb movements (Shima et al. 2000), as the neurons in the

SMA were shown to only fire to a specific sequence of movements and not for individual movement segments.

1.2.3 *Somatosensory Cortex*

The primary somatosensory cortex (S1) is located in the anterior portion of the parietal lobe and conveys the sensations of touch, temperature, pain, and limb position (proprioception) that are important in guiding movement. Proprioception originates from sensors located in muscles and joints (Golgi tendon organs, muscle spindles, etc.) and their inputs converge upon S1. Interestingly, S1 is somatotopically organized in a similar manner to M1.

1.2.4 *Posterior Parietal Cortex*

The posterior parietal cortex (PPC) is also known as a multimodal association cortex because many of the neurons in the area receive a combination of visual, auditory, and somatosensory inputs (Blatt, Andersen, and Stoner 1990; Andersen et al. 1997). There are several areas within the PPC that are important to movements such as eye saccades, coding space in head-centered coordinates, as well as the control of grasping and reaching movements. Studies have also shown evidence that the PPC receives visual information that is related to both the state of the limb and the goal of the movement (Baizer, Ungerleider, and Desimone 1991).

1.2.5 *Prefrontal Cortex*

The prefrontal cortex (PFC) is located in the frontal lobe and is thought to have a major role in high-level executive functions relating to movement (Tanji and Hoshi 2008). The PFC shows similar characteristics to PM cortex in that neurons in the PFC display direction-dependent activity related to the onset of movement. Although, these neuronal responses were found to begin approximately 150ms earlier than the neuronal responses recorded in PM cortex (di Pellegrino and Wise 1991).

1.3 NEURAL RECORDING SYSTEMS

Electrophysiology is often the preferred method to analyze brain activity due to its ability to capture a wide range of neural phenomena, from the spiking activity of individual neurons to the slower network oscillations of neural populations. The electrical nature of neuronal activity makes it possible to detect signals on electrodes at a distance from the source, but each type of recording electrode comes with its own caveats. Typical electrophysiological recording methods include those on the microscale that measure currents of single ion channels (patch-clamp), or direct measurements of intracellular voltage (microelectrode), as well as at the macroscale that measure relatively large areas of brain activity (e.g. fMRI, EEG, ECoG).

Electrodes placed closer to the brain provide greater signal than those that are placed further away such as on the surface of the scalp. Electrocorticography (ECoG) electrodes are placed directly on the exposed surface of the brain to record electrical activity from the cortex. ECoG electrodes provide a signal that is many degrees of magnitude larger than the signal recorded from surface EEG electrodes. However, ECoG electrodes are considered invasive, as they require surgery to place the electrodes on the surface of the brain.

EEG electrodes are placed on the surface of the scalp. As discussed briefly above, EEG measures the summation of inhibitory and excitatory postsynaptic potentials of populations of neurons. EEG is a neural recording technique that provides a relatively high-temporal resolution when compared to methods such as fMRI that are 2-3 orders of magnitude slower. This is one reason why EEG is a commonly used tool for measuring fast and dynamic motor neuronal processes. Another reason is that EEG measures neural population activity directly. The voltage values recorded using EEG electrodes are relative voltages, as the voltages recorded from one electrode are actually the change in electrical potential between that electrode and a reference electrode placed elsewhere on the head. A downside to EEG recordings is that it has relatively low spatial

resolution compared to fMRI techniques. The activity that is recorded below one electrode is not necessarily reflective of only the activity of the neurons directly beneath that electrode, but is likely a mixture of near and distant neuronal activity. This is in part because the signal recorded by an EEG electrode depends on the anatomy of the cortex and skull.

ECoG electrodes provide a signal that is many degrees of magnitude larger than the signal recorded from surface EEG electrodes. However, ECoG electrodes are considered invasive, as they require surgery to place the electrodes on the surface of the brain. Subdermal electrodes are placed below the scalp, but above the skull, and can be thought to provide an intermediate option in regards to the degree of invasiveness and signal quality when compared to surface EEG electrodes. Research has shown that subdermal wire electrodes maintain good recording characteristics with stable impedances for long-term monitoring of cortical neural signals.

In contrast to ECoG, EEG, and Subdermal signals, the functional magnetic resonance imaging (fMRI) BOLD (blood oxygenation level dependent) signal is a measure of hemodynamic activity and it not a direct measure of neural activity. The idea behind the fMRI BOLD signal is that there is an increase in blood flow to areas of high neuronal activity. The fMRI method is based on MR images that are sensitive to the changes in the oxygenation state of hemoglobin molecules (Ogawa et al. 1990). Hemoglobin has different magnetic properties based on the concentration of oxygen molecules that are bound to it; when it is fully saturated with oxygen molecules it behaves like a diamagnetic substance and when oxygen molecules are removed it behaves as a paramagnetic substance. Therefore, the areas of the brain containing a higher concentration of oxygen molecules will provide a higher signal than those areas with a lower concentration.

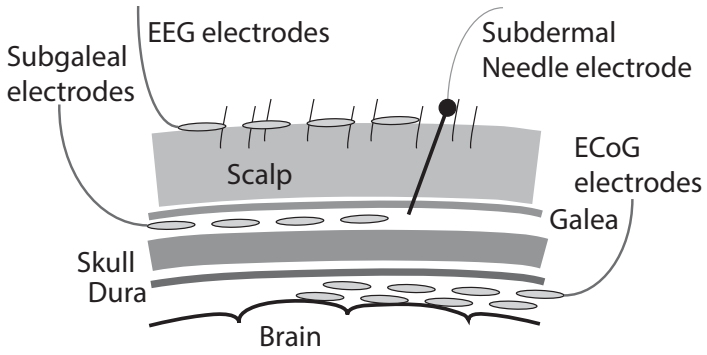

Figure 1.3. Schematic of several common electrode depths and relevant layers of anatomy. Not to scale.

Adapted from Olson et al. 2015

1.4 BRAIN-COMPUTER INTERFACES

A BCI typically focuses on utilizing the cortical signals produced by a certain area of the brain that are associated with a particular function (e.g. movement or cognitive process). The goal of the BCI is to allow a person to use these neuronal signals to control a device for communication or manipulation purposes such as a keyboard, mouse, or prosthetic limb. The cortical signals used for device control are often referred to as "signal features", which need to be extracted from extraneous content (known as noise) of the recorded cortical signal. An important measurement often used to represent how much of the desired signal features are corrupt with noise is known as the "signal-to-noise ratio (SNR)", which is simply a ratio of signal power to noise power. Therefore, a high SNR indicates that the signal of interest is minimally corrupted with background noise. The signal features that drive a BCI are often combinations or

transformations of multiple features detected at multiple time points and/or electrodes, which often represent the user's intentions more accurately.

The signals recorded for BCI control range from neuronal firing rates, or 'spikes', recorded from extracellular electrodes to frequency oscillations measured from ECoG or EEG electrodes. These oscillations are thought to reflect the rhythmic fluctuations in the excitability of neurons or population neurons and vary in their frequency, amplitude, and phase. The most common frequency oscillations utilized for BCI control are the low frequency mu (8-13 Hz) and beta oscillations (18-30 Hz) and the high frequency gamma (> 30 Hz) oscillations. During motor related tasks a decrease in amplitude known as event-related desynchronization (ERD) can be detected both invasively and non-invasively in the mu and beta frequency bands over the sensorimotor regions of the cortex. (McFarland et al. 2000; C Neuper and Pfurtscheller 2001; Christa Neuper et al. 2005). Subjects can learn to control these amplitude changes to control some feature of a BCI system such as the movement of a curser on a computer screen. The higher frequencies have been found to increase in amplitude in the sensorimotor regions with movement related tasks (C Neuper and Pfurtscheller 2001; Crone et al. 1998) and subjects have also learned to control these amplitude changes in a similar manner .

Studies have found that actual movement and imagined movements result in similar changes in brain activity (McFarland et al. 2000; K. Miller et al. 2010). Motor imagery is the mechanism by which many BCI implementations are driven and is a useful paradigm to prove the concept of a pure brain-driven device, in contrast to overt movement. In paralyzed subjects who are not capable of overt movement, imagery and attempted overt movement might be indistinguishable. Recording and using HG power from the motor cortex due to imagery in an EEG-based BCI is challenging due to the very small amplitude of the signals and the imprecise timing inherent in imagery tasks. In addition, since imagery strategies vary across trials and

subjects, one cannot expect a fixed average time course for the HG activity and thus the ability of trial averaging to improve SNR is limited.

Even in the absence of any suitable motor cortex function, a BCI user might still be capable of controlling a BCI by activation of other areas of the cortex voluntarily. An example of this is the P300 speller paradigm (Wolpaw et al. 2002; Sellers et al. 2006; Ahi et al. 2011; Belitski, Farquhar, and Desain 2011). However, unlike a motor rhythm driven BCI, this type of interface is not generally well suited for continuous feedback due to its discrete output as only one letter can be selected at a time. Thus, no continuous or graded output is possible with this paradigm. Non-motor tasks such as mental rotation, auditory imagery, and mental subtraction can modulate cortical rhythms in the alpha and beta ranges (Friedrich, Scherer, and Neuper 2012). These paradigms can provide an alternative control signal in the absence of any meaningful motor cortex signal.

1.5 EEG SIGNAL PROCESSING

1.5.1 *Data Sampling*

EEG signals are captured through a process known as sampling where the continuous analog signal is sampled at certain instants in time to capture the raw voltage values. These captured voltage values are referred to as “samples” and the rate at which the samples were captured is know as the “sampling rate”, typically measured in samples per second, or Hertz (Hz). Therefore, the higher the sampling rate the more accurately the sampled signal represents the true EEG signal. However, the true signal can be represented accurately with a minimum sampling rate known as the “Nyquist Sampling Rate”. The basis of the Nyquist sampling rate involves a discussion that goes beyond the scope of this thesis; so briefly, it is the sampling rate that is at least double the highest frequency in the analog signal.

EEG signals recorded from the brain are often on the order of microvolts (μV) and need to be amplified to levels that can be processed. Once amplified the signals are digitized, using an analog-to-digital converter, and sent to a computer. Most raw EEG data is collected in the time-domain (i.e. the signal amplitude values are viewed over time) and needs to be transformed into its equivalent frequency-domain (i.e. the amplitude and power over the range of frequencies). This transformation can be accomplished using variations of the Fourier transform, which allows us to view the frequency content of the signal.

1.5.2 *Data Filtering*

Data is often filtered in a way that modifies its frequency content by amplifying or attenuating certain frequencies in order to help remove artifacts, low-frequency drifts, or electrical line noise. The four most common filters used in EEG signal processing include low-pass, high-pass, notch, and bandpass filters. Low-pass filters attenuate high frequencies; in a similar manner high-pass filters attenuate low frequencies, often to minimize low-frequency drift. Bandpass filters preserve signal power in a specified range of frequencies, while notch filters attenuate signal power in a specified range of frequencies (it is most commonly used for attenuating 50/60 Hz line noise). Time-frequency decomposition methods apply temporal filters to the data and are discussed briefly in the section below.

1.5.3 *Artifact Detection and Removal*

An important preprocessing step prior to data analysis is to remove any trials containing artifacts that may skew the results. There are several sources of artifacts that need to be considered when recording any type of neural activity. Artifacts include interference from electrical sources such as 50/60 Hz line noise, biological artifacts from sources such as eye movement (electrooculographic; EOG), heartbeat (electrocardiographic; ECG), and muscle activity (electromyography; EMG). There are several methods that are often used to address

these types of artifacts. Line noise in the 50 or 60 Hz frequencies that is generated from electrical systems can often be removed by applying a notch filter to attenuate a narrow frequency band around the noise frequency. Attenuating artifacts generated from EMG sources is often difficult due to its broadband activity, which makes it difficult to detect and remove. The most prominent EMG activity can occasionally be removed through a manual inspection of the raw data. EOG artifacts are usually in the low frequencies (around 1 Hz) and are often fairly easily removed by applying a high-pass filter.

1.6 CORTICAL SOURCE LOCALIZATION

As mentioned previously, EEG records changes in scalp potentials due to cortical activity through a number of spatially distributed electrodes placed on the scalp. However, due in part to the attenuation of the signals as they pass through the tissue layers of the head, the spatial distribution of these recorded voltages do not accurately reflect the spatial distribution of the true cortical activity. The cortical activity can be computed from the EEG recordings by solving what is known as the inverse problem.

In order to compute an inverse solution from EEG surface recordings, a forward model is required. Forward models predict what the EEG scalp potentials would be based on the conductivity information provided by the geometry of a head model. This process of generating the forward model solely depends on the head geometry and the electrode positions and can be computed independent of the actual EEG data. The head models used in the studies outlined in this thesis were derived from the subject's individual head anatomy, which was acquired with MRI. There are several different methods that are used to model the conduction throughout the various tissues in the head. In our studies, we generated a realistic boundary element model (BEM) for each of the separate tissue compartments (skin, outer skull, inner skull, and gray/white matter interface). Another necessary component of the head model is the scalp

electrode position for each electrode. This can often be measured using a 3D localizer. The scalp electrodes and MRI derived BEM models are then co-registered based on anatomical landmarks to determine where the electrodes are positioned in relation to the brain.

With the forward model a solution to the inverse problem of localizing the cortical source activity can be computed in several ways. The most common methods for EEG source localization are minimum-norm solutions and beamformers. These spatial filters are designed as a constrained minimization problem. For example, the Linear Constrained Minimum Variance (LCMV) method (M. Yutchman 1997) is designed to pass the signal coming from a given spatial location while attenuating signals coming from other locations. This result is obtained by applying an appropriate weight vector to the signal time series in order to focus on processing individual source locations to explain the measured data while blocking signals from all other locations.

Chapter 2. DETECTION OF EEG HIGH GAMMA CORTICAL ACTIVITY DURING MOTOR IMAGERY

2.1 INTRODUCTION AND BACKGROUND

The high gamma band (70-150 Hz; HG) is a rapidly evolving, spatially localized signal (Crone et al. 1998; K J Miller et al. 2009) that is thought to be associated with local neuronal processing (Manning et al. 2009; Kai J Miller, Weaver, and Ojemann 2009). This high frequency activity has been found across the cortex reflecting local computation across a number of functional domains including sensory processing, attention, memory, and movement control. Additionally, invasive studies with electrocorticography (ECoG) have shown that motor imagery elicits HG activity in the motor cortex (K. Miller et al. 2010). Combined with the rapidly evolving, spatially constrained nature of the signal this makes HG band responses an attractive candidate for brain-computer interface (BCI) control. Unfortunately, HG activity overlaps entirely with the spectral bandwidth of muscle activity (20-300Hz) leading to artifacts from muscle activity in non-invasive electroencephalographic (EEG) recordings from the scalp. In addition, the high frequency band has a low signal-to-noise ratio (SNR) in EEG recordings due to the attenuation and smearing of electrical potentials when they diffuse through the intervening tissues (dura, skull, and scalp) to the surface recording electrode (Buzsáki, Anastassiou, and Koch 2012). Therefore, the bulk of the work done to date on HG activity has used invasive recording modalities where the SNR is greater and muscle artifacts almost non-existent.

It has recently been shown that HG activity can be detected non-invasively by electroencephalography (EEG) and magnetoencephalography (MEG). HG activity was found in the primary motor cortex prior to and during finger movements in EEG recordings (Ball et al. 2008; Dalal et al. 2008; F Darvas et al. 2010) and MEG studies have demonstrated that high

frequencies peak around 70-80 Hz in the primary motor cortex, with a bandwidth of ~40 Hz, during self-paced movements of the upper and lower limbs (Cheyne et al. 2008). These peak frequencies and bandwidth were found to vary across individuals and the limb that is moved.

During motor execution, as well as mental motor imagery, event-related desynchronization (ERD) can be detected both invasively and non-invasively in the mu (8-13 Hz) and the beta (18-30 Hz) frequency ranges (McFarland et al. 2000; C Neuper and Pfurtscheller 2001; Christa Neuper et al. 2005). The HG signals in motor cortex during motor execution and imagery have been detected using invasive modalities including ECoG (K. Miller et al. 2010) and studies have shown HG activity in the visual cortex during a mental rotation task using MEG (De Lange et al. 2008), HG activity detected from non-invasive recording methods during motor imagery has not yet been reported. Here I present an analysis of HG activity during motor imagery using non-invasive EEG in healthy subjects.

The following work was published in:

(Smith et al. 2014). Non-invasive detection of high gamma band activity during motor imagery. Front. Hum. Neurosci. 8:817

2.2 MATERIALS AND METHODS

2.2.1 *Subjects*

Data were recorded from ten healthy adult subjects (4 males, mean age=24.9 years, range=20-30 years). Nine subjects were right-handed and one subject was left-handed. Subjects gave their informed consent according to the protocol approved by the Institutional Review Board (IRB) of the University of Washington.

2.2.2 *Task*

Subjects were cued to imagine moving their fingers in a tapping sequence: pinch thumb to each digit once from proximal to distal and then ending the sequence by pinching thumb to ring-finger. Subjects imagined moving both their left and right hands. During the EEG session, subjects were seated in a recliner and 4 blocks of 25 right and 25 left hand trials were recorded, totaling 100 trials per hand. The subjects had their eyes open and fixated on a fixation cross during rest or cue during movement. Each trial consists of a rest period of 2 s, during which a fixation cross was shown. At the end of that rest period the fixation cross was changed to a written instruction, i.e. the cue, which was either "right" for right hand imagery or "left" for left hand imagery. The cue was shown for 3 s and then changed back to a fixation cross, which concluded the trial. During each block "left" and "right" cues were presented in random order, for a total of 50 cues per block.

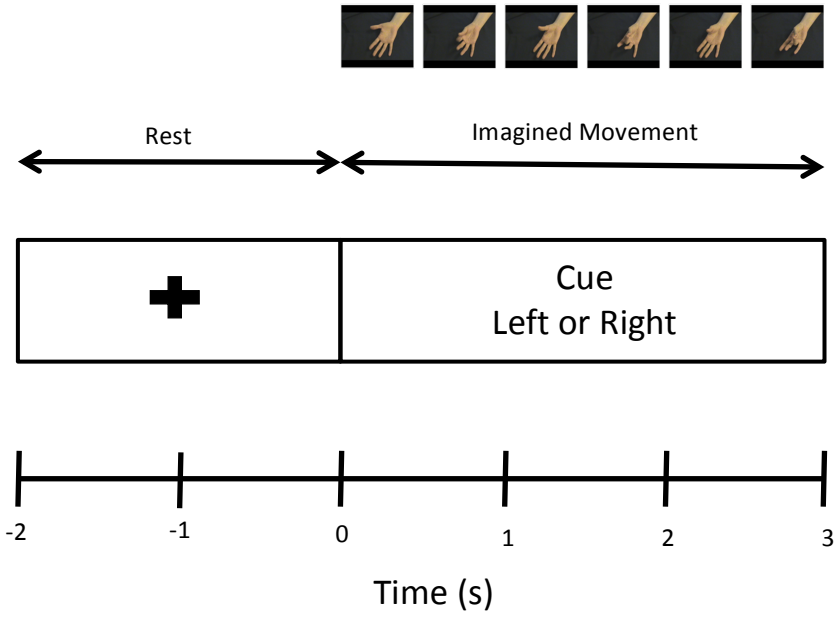

Figure 2.1. Description of motor imagery task. Right or left hand cue was randomly presented at t = 0 and persisted for 3 seconds. Subject was able to perform the motor imagery task once at any time during cue presentation. An inter-trial interval of random length between 2-3 seconds was presented as a blank screen after the cue disappeared. During which time the subject could blink or move. A rest period consisting of crosshairs centered on the screen was presented for 2 seconds just before cue onset.

2.2.3 *MRI Data Acquisition*

Scanning was conducted at 3T (Philips Achieva) using an 8-channel head-coil. For source estimation and cortical surface reconstruction, T1-weighted 3-dimensional high-resolution multi-echo MPRAGE (MEMPRAGE) structural images (with a 4 echo read out with echo times starting at 2 ms and stepped every 2 ms) and two Fast Low-Angle Shot (FLASH) sequences (Haase et al. 1986) starting at both TE 5 and 30 ms respectively (each with an echo train of 6, stepped every 2 ms) were acquired. All sequences were reconstructed into a 1^3 mm tissue space before head model reconstruction.

2.2.4 *EEG/EMG Data Acquisition*

EEG data was continuously recorded from 54 electrodes (BrainProducts 64-channel actiCAP (BrainProducts, Gilching, Germany)) during each block. The actiCap has a subset of electrodes based on the 10-20 system. A schematic of the electrode montage is shown in Fig 1. Data was sampled at 1200 Hz, using four GugerTec (GugerTec, Graz, Austria) EEG amplifiers recorded in DC, from -250 mV to +250 mV. Impedance values were kept below 20 kOhm. In parallel, we recorded at the same sampling rate the EMG (electromyogram) from the flexor indices from both hands and EOG (electrooculogram) in bipolar configurations.

A 3D localizer (Patriot, Polhemus, Colchester, VT) was used to determine the electrode positions for each subject, as well as the positions of three anatomical landmarks: nasion, and the left and right pre-auricular points.

2.2.5 *EEG/EMG Data Segmentation*

For each block, data was segmented into 5 s long segments, with time 0 s centered at the presentation of the cue, i.e. "left" or "right" hand imagery, resulting in a within-trial time axis ranging from -2 s to 3 s. The motor imagery was taking place anywhere between 0 and 3 s. The same segmentation was applied to EMG and EOG data.

2.2.6 *Head Modeling*

A 3D structural headmodel was created for each participant by averaging across all acquired echo times within the MEMPRAGE scan and incorporating 2 FLASH sequences (flip angle = 5 and 30 deg) (Figure 1). We used the FreeSurfer (http://surfer.nmr.mgh.harvard.edu/) reconstruction software for an automated segmentation of the MR images into separate tissue types and boundary surfaces, specifically *scalp, outer skull, inner skull and white matter/gray matter interface.* The white/gray matter interface served as a source space for EEG source reconstruction. The BrainStorm software package ((Tadel et al. 2011) - http://neuroimage.usc.edu/brainstorm) was then used to compute a realistic boundary element model (BEM) for each subject. The final BEM output was used to create a forward model for each subject, which is a requirement for any inverse mapping of activity from the EEG sensors to the cortex. Scalp electrode positions, measured with a Polhemus FastTrak device (Polhemus, Colchester, VT), were co-registered with the MR images and thus with the headmodel through three anatomical landmarks: nasion, left pre-auricular point, and right pre-auricular point.

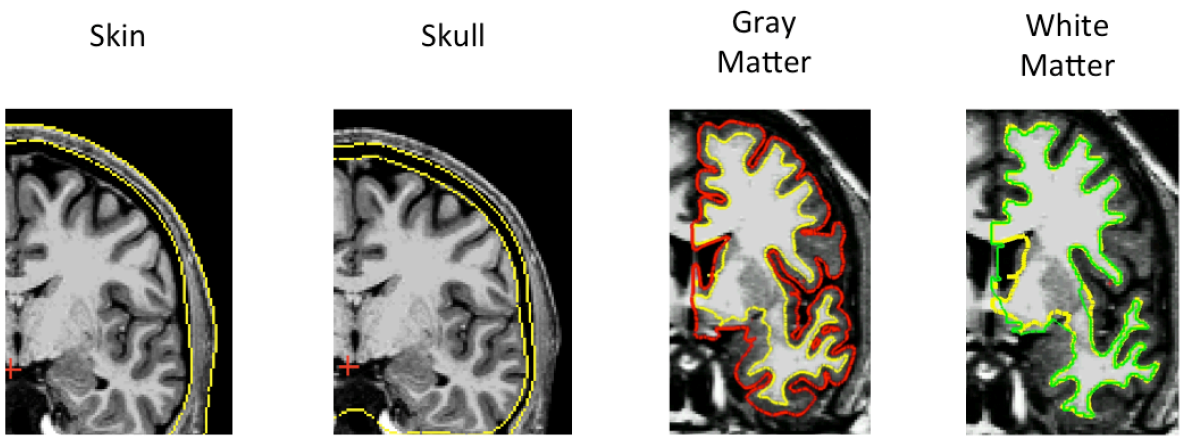

Figure 2.2. An example of an individual subject's segmented tissues from MEMPRAGE and FLASH MRI scans. Segmentation shows the boundaries of the scalp, outer skull, inner skull, and white/gray matter surfaces.

2.2.7 *Source Mapping*

We used a linearly constrained minimum variance (LCMV) beamformer to map from the EEG channel domain onto the white/gray matter interface. Similar to a minimum norm least squares (MNLS) estimate mapping, the LCMV beamformer provides a transfer matrix from channel domain to source domain, which is essential for fast computation of source maps, but produces more focal results (F Darvas et al. 2004). ECoG studies (Kai J Miller et al. 2007; Crone et al. 1998) have shown HG to be typically focal in nature and thus the LCMV provides a more accurate mapping of this focal source type than the MNLS method. Similar to (Felix Darvas, Rao, and Murias 2013), we compute a map of cortical activity for a specific frequency from a wavelet transform of the data, using the complex Morlet wavelet for the time-frequency decomposition. The beamformer weights were computed based on the broadband signal, which yields a single set of channel weights for each cortical source location, which are then applied to each of the complex wavelet transformed data. Due to the linearity of the mapping transform, the complex wavelet coefficients for a specific frequency for the channel data can be mapped into source

space by multiplication of the transfer matrix to the time by channel vector of complex coefficients, i.e.:

$$j_i(t,f) = T\, d_i(t,f),$$

where *d* is the complex wavelet transform of recorded data at time *t* and frequency *f*, *T* is the transfer matrix and *j* is the resulting cortical map of complex coefficients for the *i*th trial. The average time varying power or amplitude is then computed as:

$$p(t,f) = \sum_{i=1}^{N} |j_i(t,f)|^2 \text{(power) or}$$

$$a(t,f) = \sum_{i=1}^{N} |j_i(t,f)| \text{ (amplitude),}$$

where N is the number of trials. Here we compute amplitudes to reduce the sensitivity to outliers. We normalize the resulting cortical amplitude map with respect to a baseline interval (-1s – 0s) to equalize the amplitude differences across voxels of the map, by computing Z-scores (see Bar et al. 2006) for similar application). The Z-scores of the amplitude time series represent changes in a given frequency relative to the baseline, measured in units of the standard deviation (over time) of the baseline. Unlike a relative percent change measure, which is frequently used in ERD/S analysis, the Z-scores take into account the variability of the baseline and thus provide a more realistic assessment of the relative change.

2.2.8 *Statistical Analysis*

EEG signals, especially in the HG range, are highly susceptible to noise originating from non-cortical sources. Of particular concern is that of muscle activity (EMG), which overlaps the HG frequency range and exceeds cortically generated HG power by orders of magnitude. EMG

artifacts can arise from neck muscles, facial muscles, particularly the jaws and are difficult to control. During the course of the experiment, inevitably these artifacts will contaminate a number of trials, even in the overall absence of gross motion or position shifts of the subject. Since the sources of these artifacts are random, removal of these artifacts from the signal of interest based on stable spatial patterns across the sensors is difficult. In order to control for these artifacts, we removed any contaminated trials from the study. Unlike cortical sources, the EMG spectrum increases in power over a much wider range, thus excessive increase in power above 100 Hz, very large increases in HG power (>99 percentile of the overall HG power over time) or synchronous increases in multiple channels were identified as artifacts. Artifact contamination in the analysis of event related synchronization (ERS) is additionally confounded by the fact that we average over powers, i.e. the errors in the average due to artifacts do not cancel out. Therefore, significant changes in mean amplitude or power, in the time evolution of HG power, can easily be attributed to a single artifact contaminated trial.

To ensure the stability (across trials) and significance of HG changes during motor imagery, we applied a permutation test. We tested for a significant increase of HG amplitude during the period of the paradigm where the subject was instructed to imagine movement. Here we consider an interval from t=0s (presentation of instruction, i.e. cue, to imagine either left or right hand movement) to 1s. The permutation test has the advantage of not having to make any assumptions about the null hypothesis, i.e. HG activity during periods of non-motor imagery. Furthermore, it allows us to test for non-linear statistics of the data (here the maximum HG power change over the cortical volume and over time) and it is less sensitive to outliers in single trials, thus ensuring trial-to-trial stability of the average HG power. For the permutation test, which is described in detail in (Pantazis et al. 2005), we randomly exchange a one second interval from (-1s to 0s) of the base line with the signal interval (0s – 1s) for half of all the trials, before computing the average time varying amplitude for a given frequency across trials.

Such a surrogate signal is computed for every voxel in our cortical map. By repeating this step n times, we can build up a histogram for any statistic we wish to compute on the amplitude Z-scores. Since we postulate an increase in HG amplitude in the signal interval, we chose the maximum of the Z-score over the signal period. Since motor imagery is subject initiated, we expect onset times of any HG changes to vary substantially between subjects. By taking the maximum over the signal interval, our statistic is independent of individual variation in that period. Also, for the permutation test, we avoid having to correct resulting p-values of the test for multiple comparisons across different time points. Non invasive, scalp based approaches (F Darvas et al. 2010; Cheyne et al. 2008; Felix Darvas, Rao, and Murias 2013) have shown that HG activity in the motor system is relatively narrow band and can vary across individuals. Therefore, for the permutation test, we test over the whole band from 70 Hz to 100 Hz in 1 Hz steps and again, choose the maximum Z-score across frequencies. Finally, due to the variant spatial resolution of the inverse mapping, we also select the maximum across all voxels of the map, i.e. the whole cortex. By building a histogram over the maximum in time, frequency, and space, we avoid having to correct the resulting p-values for any multiple comparisons. The permutation test also implicitly examines trial-to-trial stability of the average. That is, since any outlier trial with large HG power in the signal interval, which could cause the average HG power to be high as well, has a 50% chance of being permuted with a baseline segment and would skew the baseline HG power distribution in the same manner, the resulting average power would consequently no longer be in the tail end of the baseline distribution. Therefore, increases in the average HG power over trials in the signal period due to outliers will be tested as non-significant.

2.2.9 *EMG/EOG Data Processing*

EMG and EOG are sources of noise in the HG band and can exceed the cortical signal considerably. EOG electrodes were placed approximately 1 cm above the left and right brows and 1 cm below left and right eyes. Through the permutation test on the EEG data, we can make

sure that any significant HG effects observed in the data are not due to transient, non- stimulus induced HG activity originating from either EMG or EOG. However, any stimulus-induced, systematic EMG or EOG activity that would introduce an artifact into the EEG would still pass the permutation test. In order to rule out such systematic contamination, we compute the average EMG and EOG HG power over all trials. This was then subsequently entered into the EEG source analysis to identify systematic increases in HG in the EMG and EOG channels. Since EMG and EOG are typically of broadband nature, in the range from 70-100 Hz, we band pass filtered both signal types for each subject and side and computed the mean amplitude from the Hilbert transform of the 70-100 Hz filtered signals. Because the human brain's power spectrum recorded non-invasively hits the noise floor at around 100 Hz, this 70-100 Hz band pass filter was applied to EEG recordings.

2.1 RESULTS

2.1.1 *HG EEG Activity*

EEG and MRI data were collected on separate days in the same group of ten subjects (see Figure 2.3 for the EEG montage used).

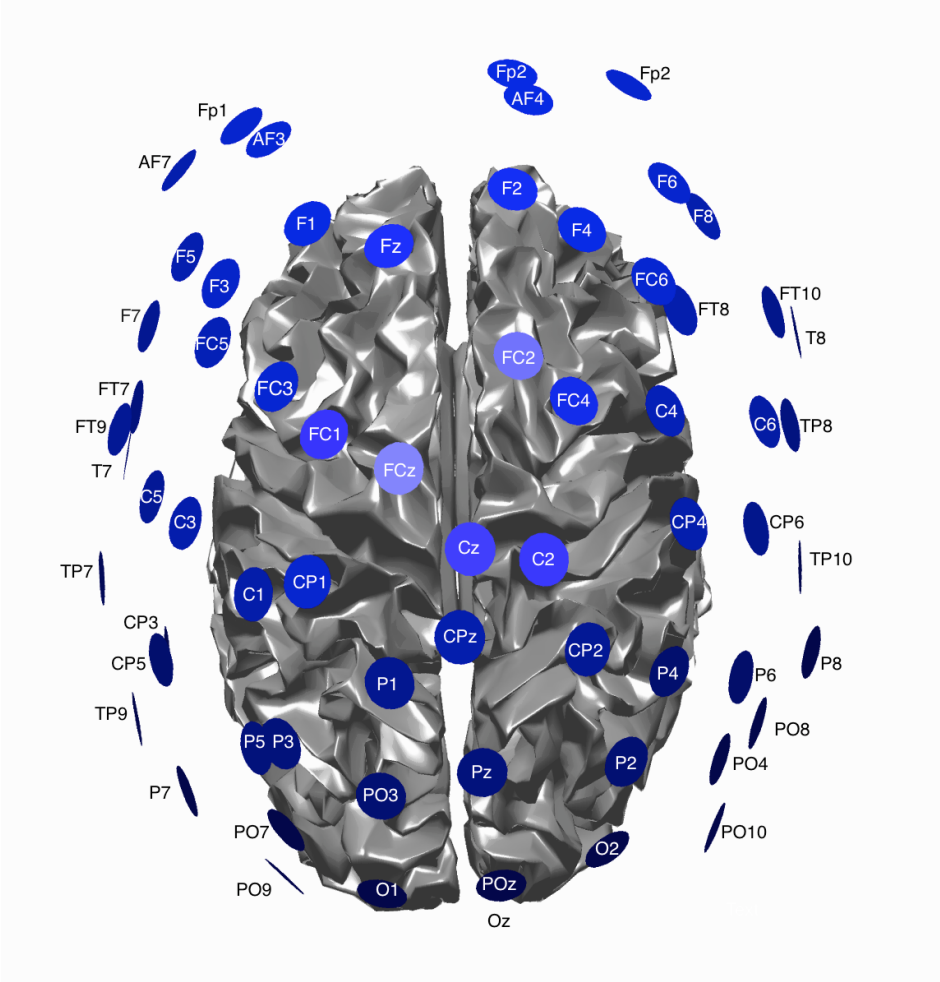

Figure 2.3. Schematic view of the EEG montage and cortical surface used for EEG data acquisition.

The ***only*** significant task induced EMG activity between 0 and 2000 ms after motor imagery cue onset was found in subject 4 (Figures 2.4 & 2.5). There was significant increase in EOG activity in subject 5 after 2000 ms, but also not overlapping with any cortical HG activity (Figures 2.5 & 2.6).

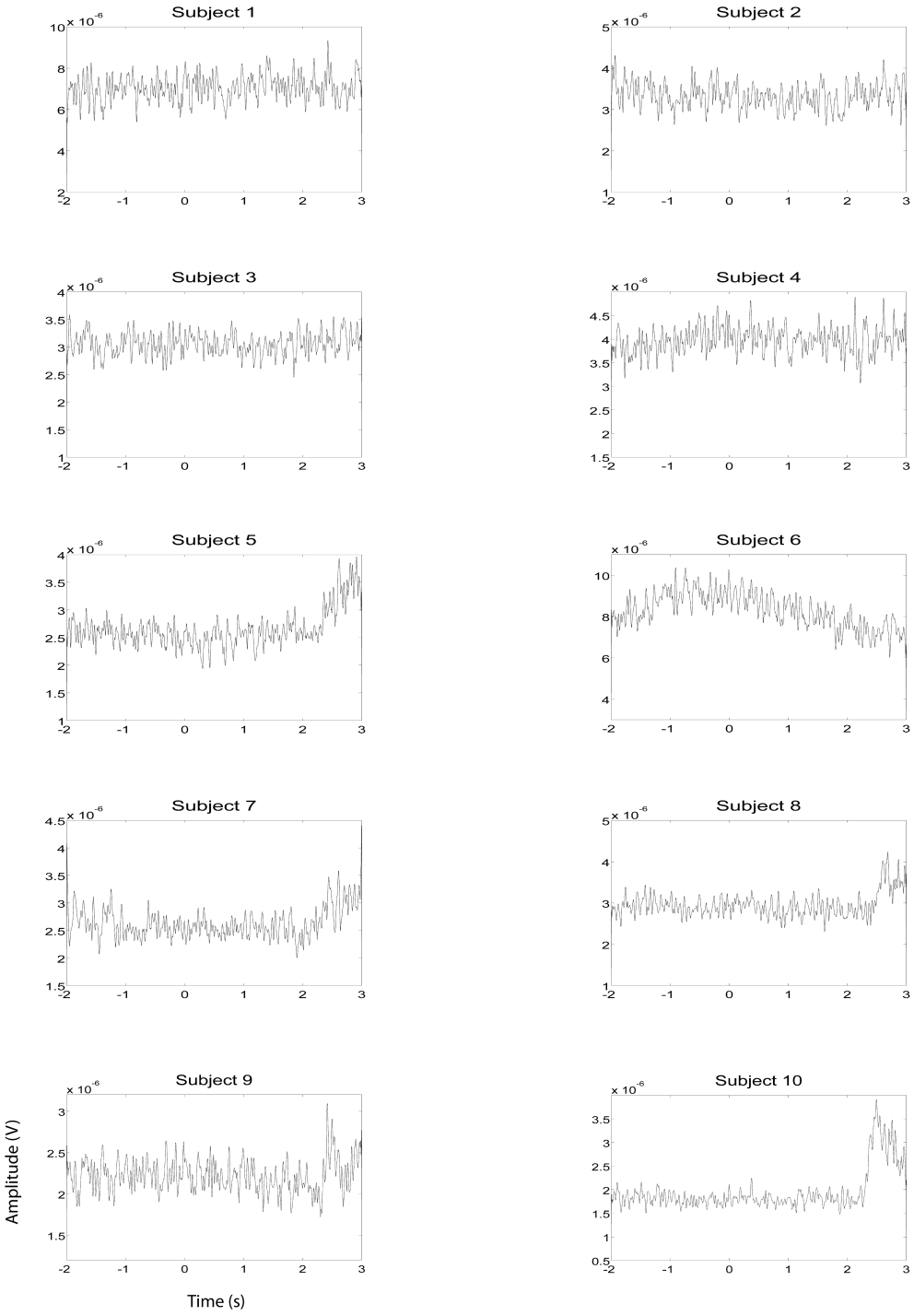

Figure 2.4. EMG HG magnitude of the left hand during left hand motor imagery. EEG recording sessions (n=10). EMG activity was averaged over all trials that were not contaminated by artifacts.

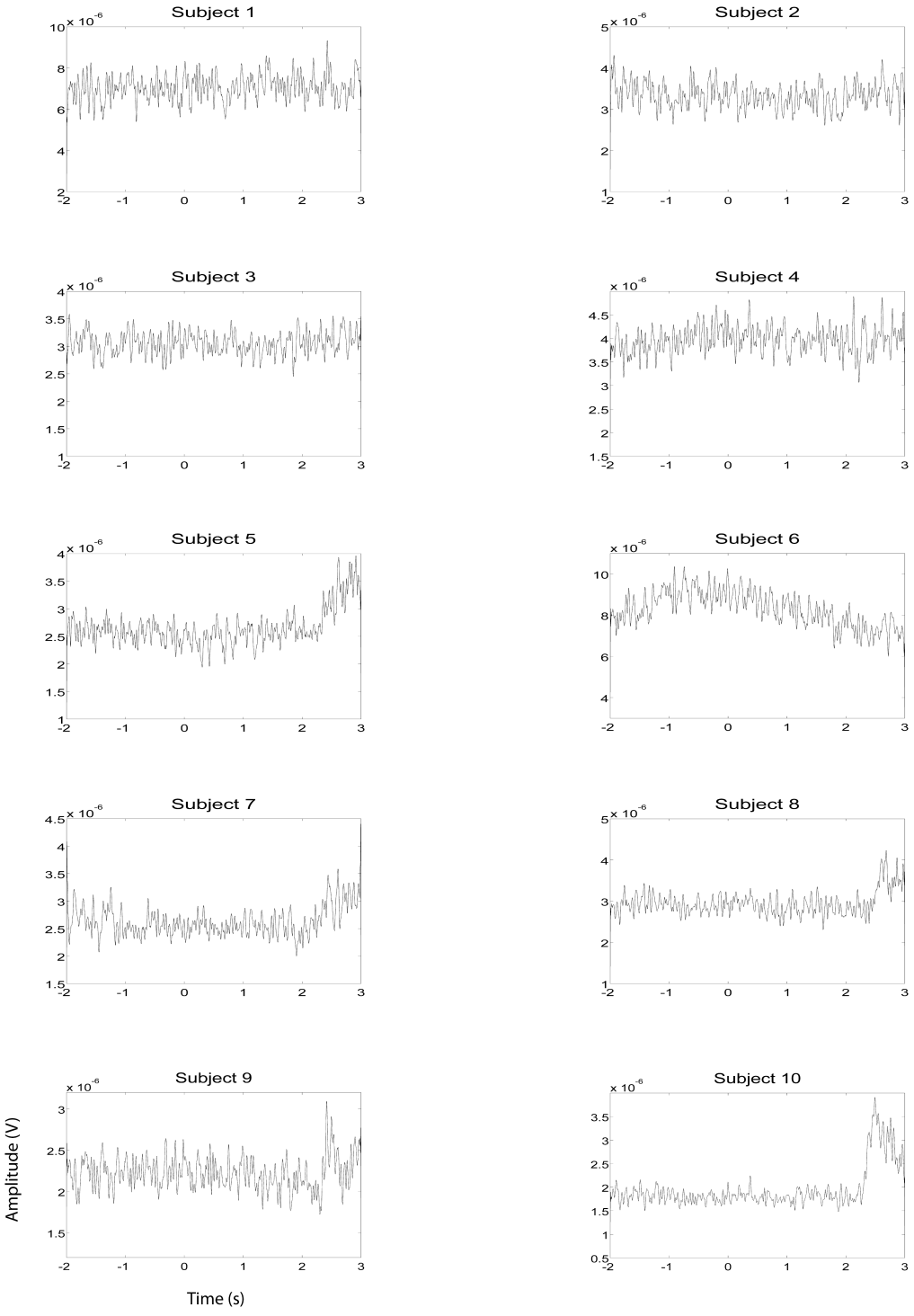

Figure 2.5. EMG HG magnitude of the right hand during right hand motor imagery EEG recording sessions (n=10). EMG activity was averaged between all trials that were not contaminated by artifacts.

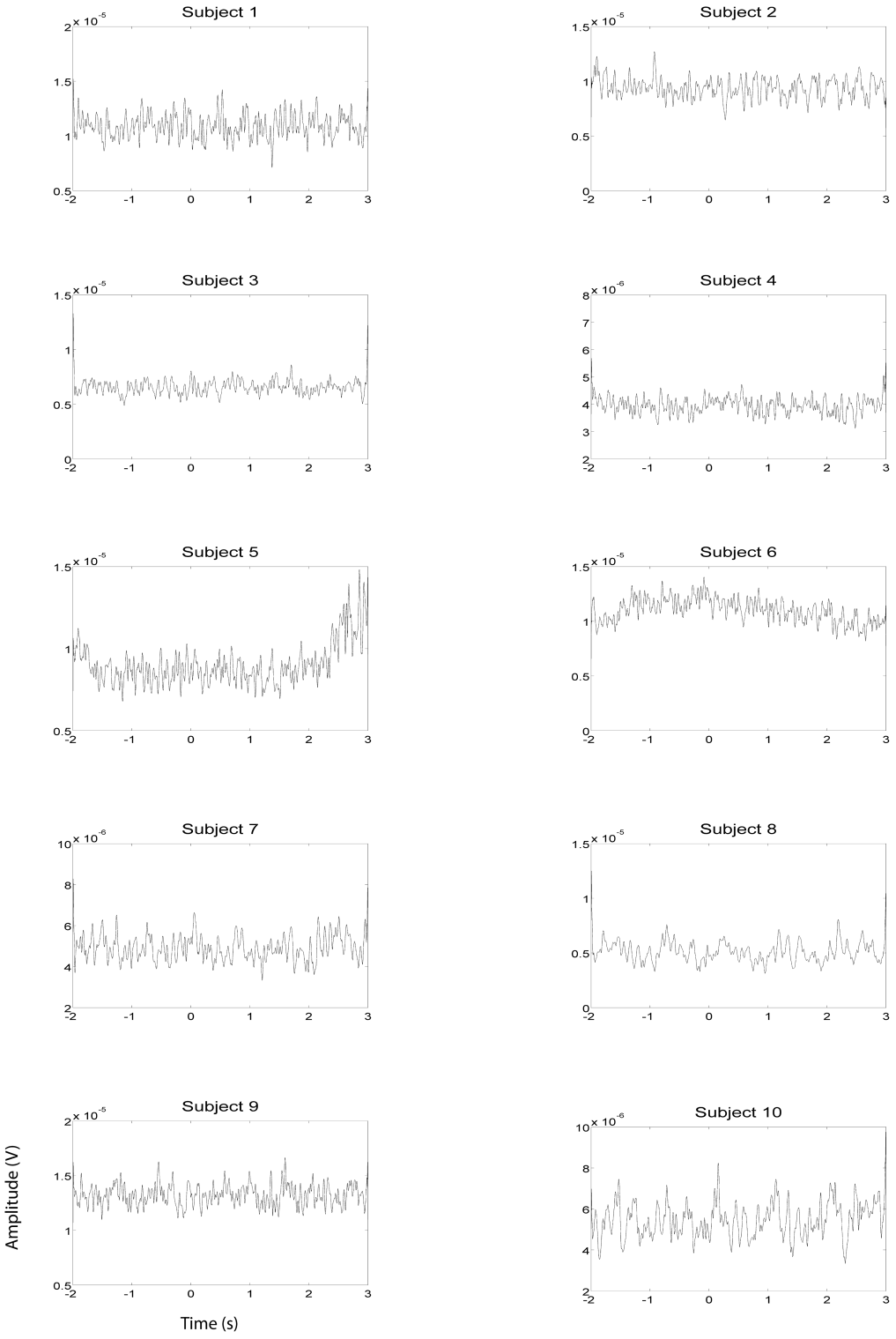

Figure 2.6. EOG HG magnitude during left hand EEG motor imagery recording sessions (n=10). EOG activity was averaged over all trials that were not contaminated by artifacts.

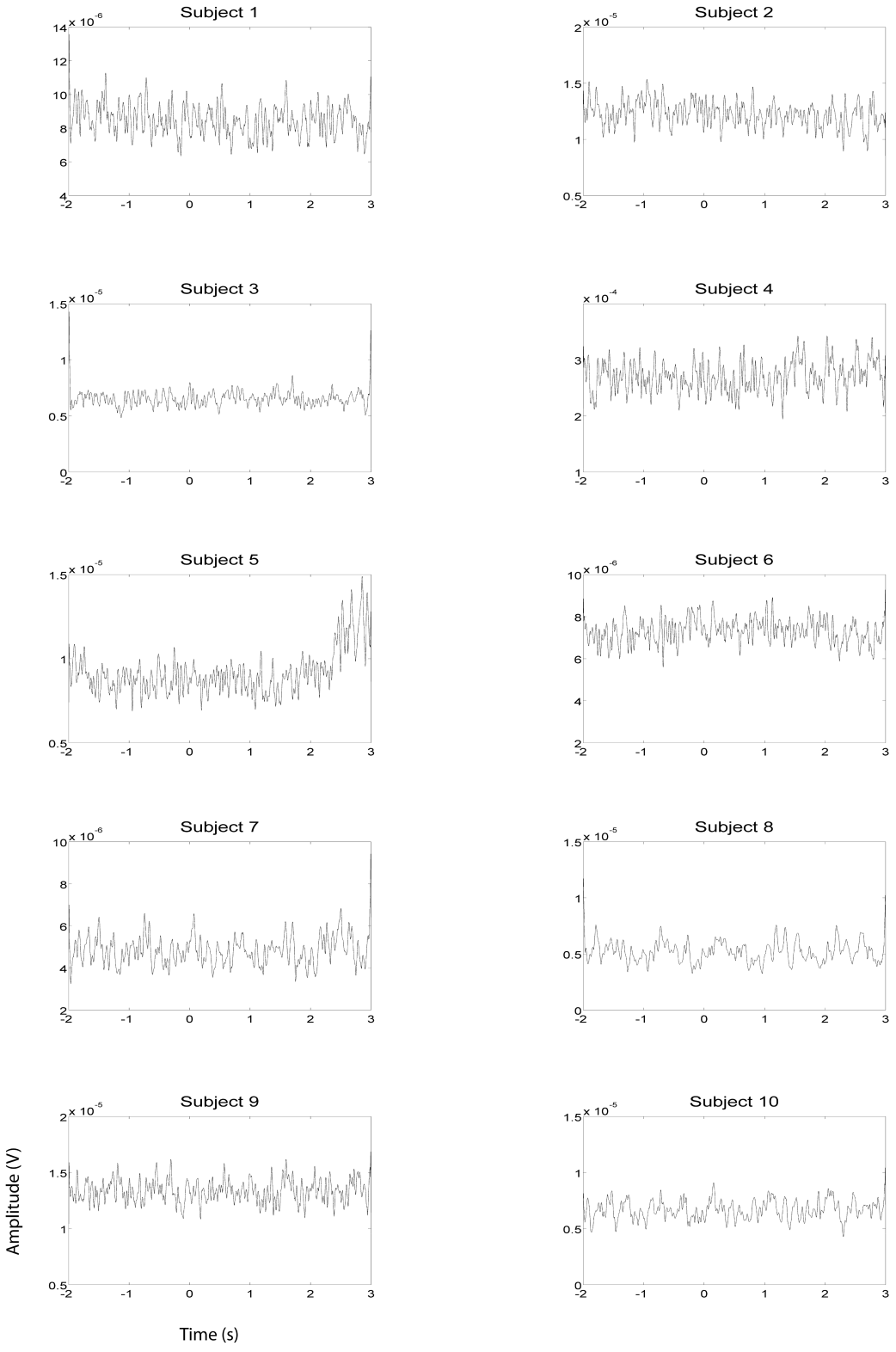

Figure 2.7. EOG HG magnitude during right hand EEG motor imagery recording sessions (n=10). EOG activity was averaged over all trials that were not contaminated by artifacts.

Significant HG increases were found to occur between 0.3s to 1.0s during the task period. Baseline was selected from -1s to 0s and the cortical distributions of relative change in the HG band were determined. Peak HG frequencies for each subject are shown in Table 1. Time-frequency representations were computed for each individual subject for the most significant voxel in the cortex after motor imagery cue onset (Subjects 5 and 8 shown in fig. 9. The remaining 8 subjects are shown in fig. 10 and fig. 11). Subjects showed significant HG activity in narrow bands that were centered between 70 and 90 Hz. In addition, most subjects showed a decrease in beta band activity that preceded power increases in the HG band, at the sites of HG activity. Because this result is commonly noted during motor imagery tasks and replicates a well-characterized phenomenon (F Darvas et al. 2010) it is likely an additional indicator that the recorded HG activity is of genuine cortical origin. Group averages of this beta band decrease are shown as cortical representations in fig. 12.

Table 2.1. Peak HG frequencies between cue onset and 1s post cue onset during left hand (LH) and right hand (RH) motor imagery EEG sessions.

Subject	Handedness	Age	Gender	Imagined Hand	Frequency (Hz)
1	R	29	M	LH	84
				RH	87
2	R	26	F	LH	79
				RH	84
3	R	26	F	LH	85
				RH	81
4	R	30	M	LH	78
				RH	78
5	R	25	F	LH	87
				RH	90
6	L	20	F	LH	82
				RH	82
7	R	30	F	LH	85
				RH	88
8	R	20	M	LH	84
				RH	88
9	R	22	M	LH	96
				RH	89
10	R	21	F	LH	89
				RH	94

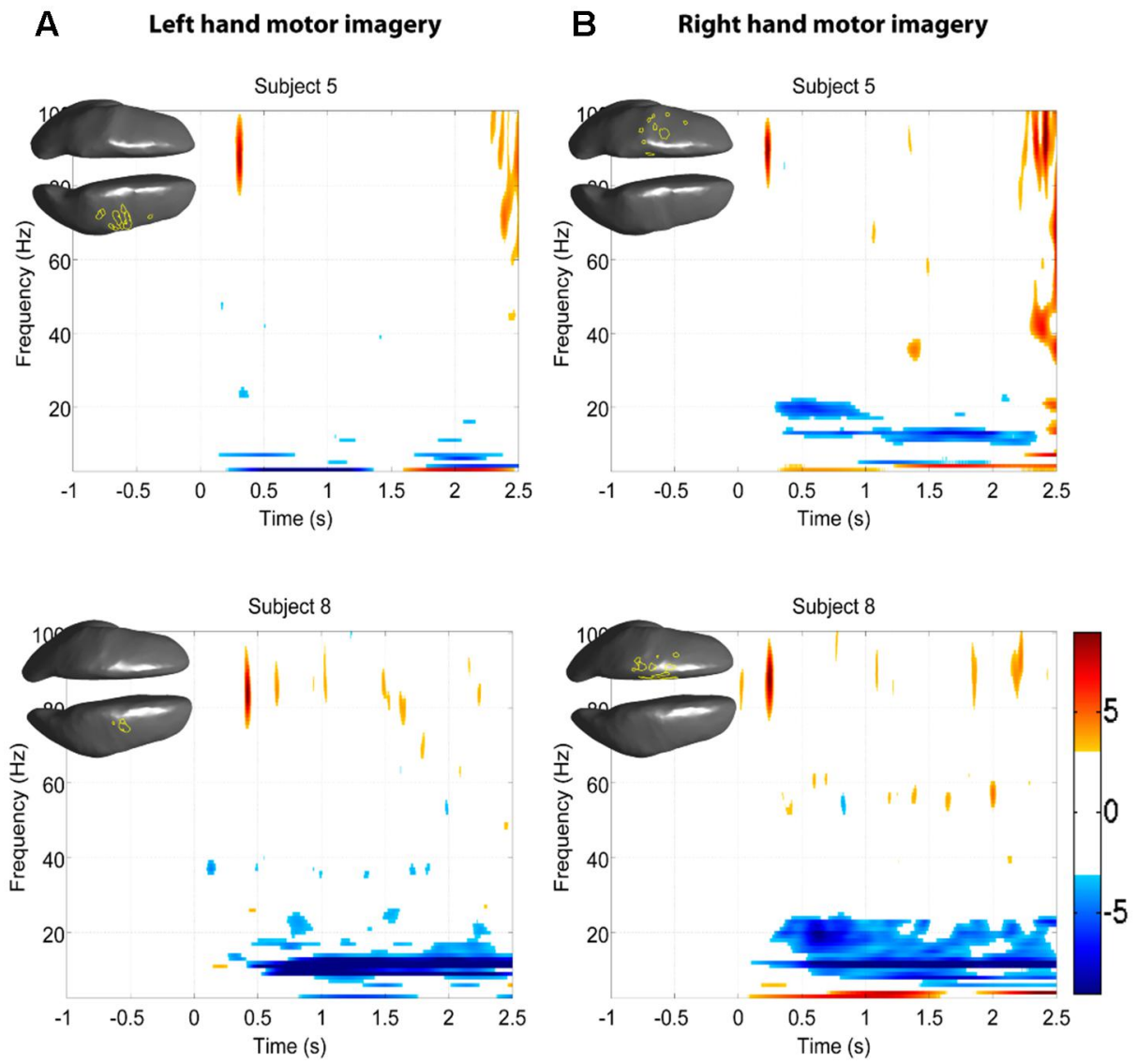

Figure 2.8. Z-score time-frequency maps for subjects 5 and 8 for the cortical regions indicated on the cortical surface displayed in the upper left corner. The maps show that subjects have significant HG increases post-cue in a narrow band. A) Time-frequency maps during left hand motor imagery. B) Time-frequency maps during right hand motor imagery.

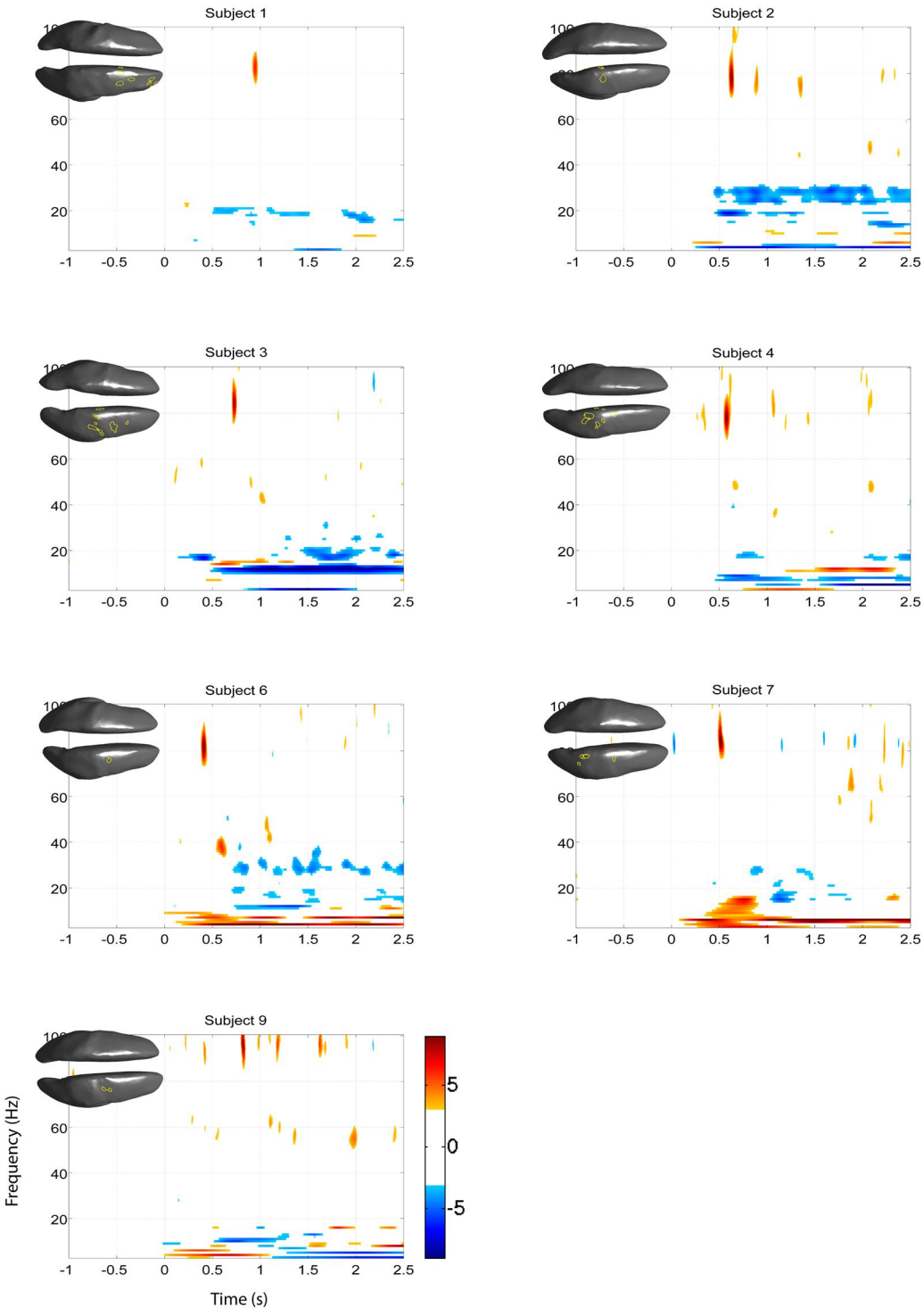

Figure 2.9. Z-score time-frequency maps during left hand motor imagery of the 8 remaining subjects for the cortical regions indicated on the cortical surface displayed in the upper left corner. The maps show that subjects have significant HG increases post-cue in a narrow band.

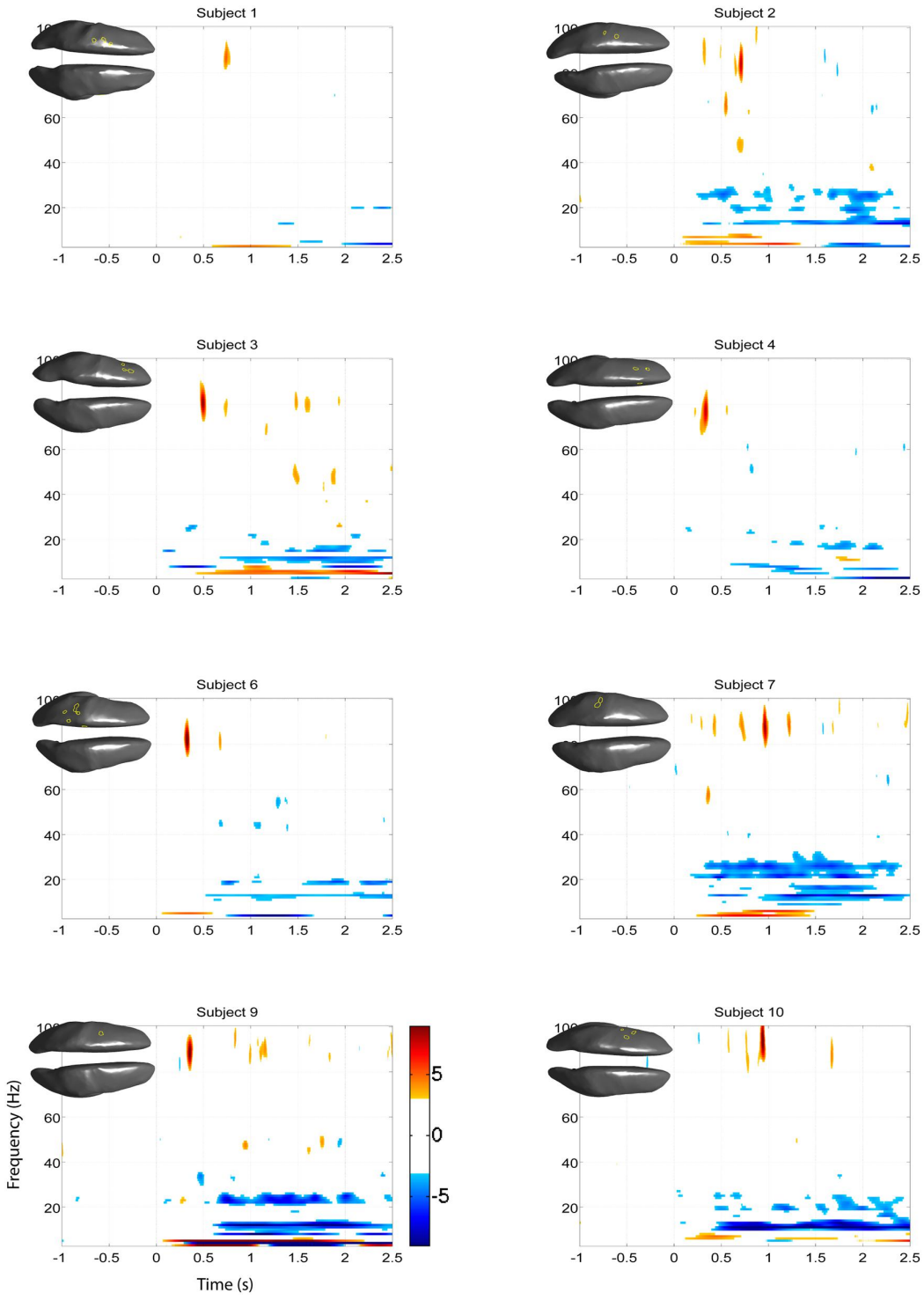

Figure 2.10. Z-score time-frequency maps during right hand motor imagery of the 8 remaining subjects for the cortical regions indicated on the cortical surface displayed in the upper left corner. The maps show that subjects have significant HG increases post-cue in a narrow band.

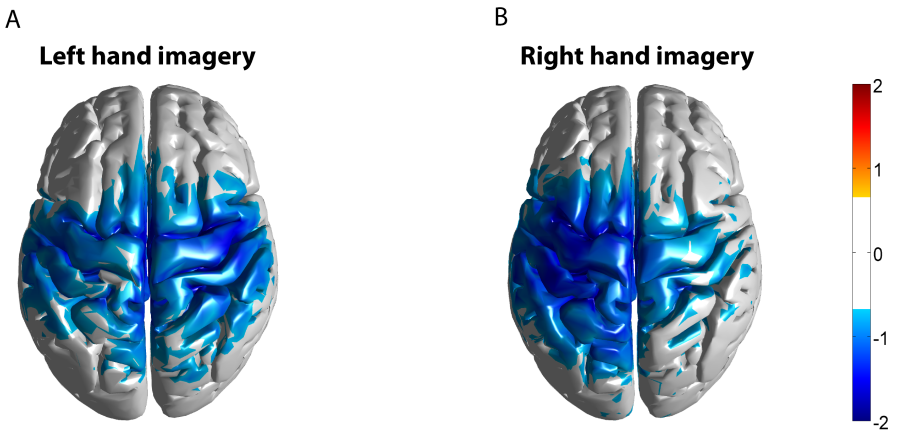

Figure 2.11. Z-score group average maps of beta band activity (15-35 Hz) of all subjects (n=10). Activity was mapped in Montreal Neurological Institute (MNI) space. A) Averaged beta activity during left hand motor imagery. B) Averaged beta activity during right hand motor imagery. The threshold for the group average was set at Z=0.72, corresponding to 2.3 in a normal distribution or a 99% confidence level.

2.2 DISCUSSION

Our results show that HG activity during motor imagery can be recovered with EEG using an individual subject's anatomical head model and inverse modeling methods. This high frequency spectral power change has been shown to correlate directly with firing rate (Whittingstall and Logothetis 2009; Manning et al. 2009; K J Miller et al. 2009) and has been demonstrated to reflect broad spectral changes across all frequencies (Kai J Miller et al. 2007; K J Miller et al. 2009).

Taken together, these results suggest that EEG can accurately resolve spatially specific estimates of local cortical high frequency signals, potentially opening an avenue for characterizing HG

signals from diverse sets of neurologically impaired populations, including various neurodegenerative disorders. Research shows that event-related oscillations in alpha, beta, gamma, delta, and theta frequency bands are highly modified in pathological brains, especially in patients with cognitive impairment (Başar et al. 2012; Basar-Eroglu, Schmiedt-Fehr, and Mathes 2012; Yener and Bajar 2012; Ozerdem et al. 2012; Vecchio et al. 2013; Yener and Basar 2012). Non-invasive EEG signals in these subject populations are currently only detected up to the beta frequency range, oscillations that are focally non-specific and likely represent an amalgamated signature of numerous anatomical substrates. There is growing evidence supporting the idea that disorders such as Alzheimer's disease target specific and functionally connected neuronal networks (Reid and Evans 2013). Thus, the non-invasive resolution of HG signals, which are believed to represent the activation of focal neural populations, may provide insights into specific neurophysiology mechanisms underlying neurodegenerative disorders such as Parkinson's and Alzheimer's. These gamma modulations could prove to be a useful electrophysiological biomarker to examine the pathophysiology of such neurological diseases.

HG EEG activity related to motor imagery

Frontal eye fields (FEF) in the prefrontal cortex are thought to play a key role in the planning and execution of saccadic eye movements, as well as visual selective attention (Bullier 2001; Russo and Bruce 1994). MEG studies have indicated that early HG activity over the right FEF is present during saccade preparation. During saccade execution, HG activity is observed in the supplementary eye fields (SEF), then subsequently progresses to the visual cortex and FEF bilaterally (Hinkley et al. 2011). In addition to FEF, it has been suggested that transient increases in scalp EEG gamma band power (above 30 Hz) in the parietal-occipital cortex can be linked to task-related saccadic eye movements (Reva and Aftanas 2004; Yuval-Greenberg et al. 2008; Trujillo et al. 2005). Yuval-Greenberg and colleagues (2008) showed data that indicates the broadband (30-90 Hz) and transient (between 200-300 ms) gamma activity recorded with EEG in the parietal-occipital cortex mirrors eye movements following the display of a new image and

that this gamma signal may be the consequence of associated ocular muscle artifacts engendered from miniature saccades. Invasive studies showed that saccadic ocular muscle activity might generate gamma-range artifacts in ECoG data that is confined to the medial temporal pole and is likely due to its immediate vicinity to the lateral rectus eye muscle (Jerbi et al. 2009). The results from the present study do not show significant increases in HG activity during the cued baseline period, indicating that the HG activity we see after cued motor imagery onset is related to motor imagery and not activity induced during miniature saccades.

HG EEG as a control signal for brain-computer interface

In the sensorimotor areas of the cortex, motor imagery has been found to be associated with increases in the HG band, as well as decreases in the beta and mu bands. Because these cortical rhythms can be intentionally modulated by motor imagery, they have been used in non-invasive (i.e. mu and beta) (Pfurtscheller et al. 2003; Pfurtscheller and Neuper 2006) and invasive (HG, mu and beta) brain-computer interface studies as a control signal (Leuthardt et al. 2006). In addition to control signals, motor imagery-based BCIs have recently shown great potential for restoring lost function and inducing activity-dependent brain plasticity in patients suffering from paralysis due to stroke (Bai et al. 2008; Buch et al. 2008; Bundy et al. 2012). However, current non-invasive motor imagery-based BCI research has been based on the low spatial resolution offered by EEG/MEG electrodes and spatially broad mu and beta rhythms, resulting in unreliable and coarse BCI control with average information transfer rates in the range 10-20 bits/min for motor-imagery BCIs (Rao 2013). The overall efficacy of these systems is limited due to the time it takes for the low frequency rhythm's amplitudes to evolve, which is on the order of several hundred milliseconds (Pfurtscheller and Lopes da Silva 1999). Ideally, a smaller response lag is desired, i.e. 100 ms or less, to ensure a more fluid alternative for device control and rehabilitation. The HG rhythms that we were able to detect in this study, with their increased spatiotemporal resolution and greater task specificity, have the potential to enhance the performance of EEG-driven orthotic and prosthetic devices by allowing the brain to interact

with assistive devices on a more natural timescale. In addition, the demonstrated ability to detect HG changes offline and non-invasively, a major strength of using EEG, will enable the development of paradigms that allow the neurophysiological functions in humans to be studied non-invasively on a more global scale compared to ECoG.

Chapter 3. CORRELATION BETWEEN EEG HG AND FMRI BOLD ACTIVITY

3.1 INTRODUCTION AND BACKGROUND

In order to examine the relationship between fMRI and the underlying neurophysiological responses several studies have compared local field potentials (LFPs), single-unit, and multi-unit spiking activity in functionally relevant areas of cortex with blood-oxygen-level-dependent (BOLD) signal responses (Logothetis et al. 2001; Mukamel et al. 2005; Niessing et al. 2005). These studies found a positive correlation between the high frequency power changes in the LFPs and BOLD signal changes. However, the cortical regions surrounding the functionally relevant areas were not examined and it is unclear whether these regions have neurophysiological correlates as well. It may be expected that they do because typical BOLD activity maps display large BOLD signal changes in cortical areas known to be related to the behavior being performed, as well as weaker, more variable signal changes in the surrounding areas (Rombouts et al. 1997; Saad et al. 2003).

Two recent studies (Conner et al. 2011; Hermes et al. 2012) examined the correlation of the BOLD signal and spectral power changes measured by ECoG. Hermes and colleagues (Hermes et al. 2012) found that spectral power increases in the high frequency range co-localized with spatially focal BOLD peaks on primary sensorimotor areas, while Conner et al. (2011) showed a positive correlation between BOLD activity and HG in pre and post central cortical areas (i.e. covering motor areas) and negative correlations with the beta frequency band.

However, ECoG recordings only provide a limited neurophysiological correlation because they do not record from the whole brain. Non-invasive studies with simultaneous EEG and fMRI have reported negative correlations with BOLD in the low frequency (4-30 Hz) range of the spectrum (Yuan et al. 2010), but the spatial association between whole-brain HG band neural

activity detected by EEG and the hemodynamic changes of the fMRI BOLD signal has not been reported. The remainder of this chapter presents an analysis comparing the HG activity measured non-invasively with EEG and the BOLD response measured with fMRI for a motor imagery paradigm.

The following work was published in:

(Smith et al. 2014). Non-invasive detection of high gamma band activity during motor imagery. Front. Hum. Neurosci. 8:817

3.2 MATERIALS AND METHODS

3.2.1 *Subjects*

Data were recorded from the same population of ten healthy adult subjects (4 males, mean age=24.9 years, range=20-30 years) mentioned in chapter 2. Nine subjects were right-handed and one subject was left-handed. Subjects gave their informed consent according to the protocol approved by the Institutional Review Board (IRB) of the University of Washington.

3.2.2 *Task*

For both fMRI and EEG sessions, subjects were cued to imagine moving their fingers in a tapping sequence: pinch thumb to each digit once from proximal to distal and then ending the sequence by pinching thumb to ring-finger. Subjects imagined moving both their left and right hands. During the EEG session, subjects were seated in a recliner and 4 blocks of 25 right and 25 left hand trials were recorded, totaling 100 trials per hand. The subjects had their eyes open and fixated on a fixation cross or cue. Each trial consists of a rest period of 2 s, during which a fixation cross was shown. At the end of that rest period the fixation cross was changed to a written instruction, i.e. the cue, which was either “right” for right hand imagery or “left” for left hand imagery. The cue was shown for 3 s and then changed back to a fixation cross, which

concluded the trial. During each block “left” and “right” cues were presented in random order, for a total of 50 cues per block.

3.2.3 *MRI/fMRI Data Acquisition*

Scanning was conducted at 3T (Philips Achieva) using an 8-channel head-coil. For source estimation and cortical surface reconstruction, T1-weighted 3-dimensional high-resolution multi-echo MPRAGE (MEMPRAGE) structural images (with a 4 echo read out with echo times starting at 2 ms and stepped every 2 ms) and two Fast low-angle shot (FLASH) sequences (Haase et al. 1986) starting at both TE 5 and 30 ms respectively (each with an echo train of 6, stepped every 2 ms) were acquired. All sequences were reconstructed into a 1 mm tissue space before head model reconstruction.

Whole brain functional images for each task-based scan were collected using a gradient echo T2* weighted sequence (TE/TR = 21/2000 ms, matrix size 80x80). Subjects participated in a standard block-designed fMRI task of imagined movement, with randomly presented blocks of left & right imagery as well as rest. A total of 15 blocks were presented, with each conditional block being presented 5 times. No condition was repeated. Each block consisted of 10 visually presented cues (left, right or rest) in the center of the screen for 2 seconds followed by a 2 second inter-trial interval. Each block lasted for 40 sec. The experiment began and terminated with a 40 sec rest period.

3.2.4 *EEG/EMG Data Acquisition*

EEG data was continuously recorded from 54 electrodes (BrainProducts 64-channel actiCAP (BrainProducts, Gilching, Germany)) during each block. The actiCap has a subset of electrodes based on the 10-20 system. A schematic of the montage is shown in Fig 1. Data was sampled at 1200 Hz, using four GugerTec (GugerTec, Graz, Austria) EEG amplifiers recorded in DC, from -

250 mV to +250 mV. Impedance values were kept below 20 kOhm. In parallel, we recorded at the same sampling rate the EMG (electromyogram) from the flexor indices from both hands and EOG (electro-oculogram) in bipolar configurations.

A 3D localizer (Patriot, Polhemus, Colchester, VT) was used to determine the electrode positions for each subject as well as the positions of three anatomical landmarks: nasion, and the left and right pre-auricular points.

3.2.5 *EEG/EMG Data Segmentation*

For each block, data was segmented into 5 s long segments, with time 0 s centered at the presentation of the cue, i.e. "left" or "right" hand imagery, resulting in a within-trial time axis ranging from -2 s to 3 s. The motor imagery was taking place anywhere between 0 and 3 s. The same segmentation was applied to EMG and EOG data.

3.2.6 *Head Modeling*

A 3D structural headmodel was created for each participant by averaging across all acquired echo times within the MEMPRAGE scan and incorporating 2 FLASH sequences (flip angle = 5 and 30 deg). We used the FreeSurfer (http://surfer.nmr.mgh.harvard.edu/) reconstruction software for an automated segmentation of the MR into separate tissue types and boundary surfaces, specifically *scalp, outer skull, inner skull and white matter/gray matter interface.* The latter served as a source space for EEG source reconstruction. The BrainStorm software package ((Tadel et al. 2011) - http://neuroimage.usc.edu/brainstorm) was then used to compute a realistic boundary element model (BEM) for each subject. The final BEM output was used to create a forward model for each subject, which is a requirement for any inverse mapping of activity from the EEG sensors to the cortex. Scalp electrode positions, measured with a Polhemus FastTrak device (Polhemus, Colchester, VT), were co-registered with the MR images

and thus with the headmodel through three anatomical landmarks: nasion, left pre-auricular point, and right pre-auricular point.

3.2.7 *Source Mapping*

We used a linearly constrained minimum variance (LCMV) beamformer to map from the EEG channel domain onto the white/gray matter interface. Similar to a minimum norm least squares (MNLS) estimate mapping, the LCMV provides a transfer matrix from channel domain to source domain, which is essential for fast computation of source maps, but produces more focal results (F Darvas et al. 2004). ECoG studies (Kai J Miller et al. 2007; Crone et al. 1998) have shown HG to be typically focal in nature and thus the LCMV provides a more accurate mapping of this focal source type than e.g. the MNLS method. Similar to (Felix Darvas, Rao, and Murias 2013), we compute a map of cortical activity for a specific frequency from a wavelet transform of the data, using the complex Morlet wavelet for the time-frequency decomposition. The beamformer weights were computed based on the broadband signal, which yields a single set of channel weights for each cortical source location, which are then applied to each of the complex wavelet transformed data. Due to the linearity of the mapping transform, the complex wavelet coefficients for a specific frequency for the channel data can be mapped into source space by multiplication of the transfer matrix to the time by channel vector of complex coefficients, i.e.:

$$j_i(t,f) = T\, d_i(t,f),$$

where d is the complex wavelet transform of recorded data at time t and frequency f, T is the transfer matrix and j is the resulting cortical map of complex coefficients for the ith trial. The average time varying power or amplitude is then computed as:

$$p(t,f) = \sum_{i=1}^{N} |j_i(t,f)|^2 \text{(power) or}$$

$$a(t,f) = \sum_{i=1}^{N} |j_i(t,f)| \text{ (amplitude),}$$

where N is the number of trials. Here we compute amplitudes, to reduce the sensitivity to outliers. We normalize the resulting cortical amplitude map with respect to a baseline interval (-1s – 0s) to equalize the amplitude differences across voxels of the map by computing Z-scores (see (Bar et al. 2006) for similar application). The Z-scores of the amplitude time series represent changes in a given frequency relative to the baseline, measured in units of the standard deviation (over time) of the baseline. Unlike a relative percent change measure, which is frequently used in ERD/S analysis, the Z-scores take into account the variability of the baseline and thus provide a more realistic assessment of the relative change.

3.2.8 *Statistical Analysis*

fMRI/MRI

fMRI data processing was carried out using FEAT (FMRI Expert Analysis Tool) Version 5.98, part of FSL (FMRIB's Software Library, www.fmrib.ox.ac.uk/fsl). The preprocessing pipeline included motion correction, high-pass temporal filtering for removal of liner drift, a spatial filter of 5 mm full-width half maximum (FWHM) and a pre-whitening filter to remove signal autocorrelations throughout the time-course. BOLD responses were estimated on an individual subject basis by applying a box-car, general-linear model design with a standard hemodynamic response convolution. Whole-brain BOLD activity was contrasted between active (left or right) and rest periods, converted into Z-scores and with a threshold at $Z > 2.3$ (uncorrected). Clusters of significant activity were masked into regions of interest (ROIs). For each participant, all functional data sets were co-registered into native MPRAGE space using a rigid-body (6 degrees of freedom) registration and trilinear interpolation.

EEG

EEG signals, particularly in the HG range, are highly susceptible to noise originating from non-cortical sources. Of particular concern is that of muscle activity (EMG), which overlaps the HG frequency range and exceeds cortically generated HG power by orders of magnitude. EMG artifacts can arise from neck and facial muscles, particularly muscles in the jaws, and are difficult to control. During the course of the experiment, inevitably these artifacts will contaminate a number of trials, even in the overall absence of gross motion or position shifts of the subject. Since the sources of these artifacts are random, removal of these artifacts from the signal of interest based on stable spatial patterns across the sensors is difficult. In order to control for these artifacts, we remove any contaminated trials from the study. Unlike cortical sources, the EMG spectrum increases in power over a much wider range, thus excessive increase in power above 100 Hz, very large increases in HG power (>99 percentile of the overall HG power over time) or synchronous increases in multiple channels were identified as artifacts. Artifact contamination in the analysis of event related synchronization (ERS) is additionally confounded by the fact that we average over powers, i.e. the errors in the average due to artifacts do not cancel out. Therefore significant changes in mean amplitude or power, e.g.in the time evolution of HG power can easily be attributed to a single artifact contaminated trial.

To ensure the stability (across trials) and significance of HG changes during motor imagery, we applied a permutation test. We tested for a significant increase of HG amplitude during the period of the paradigm where the subject was instructed to imagine movement. Here we consider an interval from t=0s (presentation of instruction, i.e. cue, to imagine either left or right hand movement) to 1 s. The permutation test has the advantage of not having to make any assumptions about the null hypothesis, i.e. HG activity during periods of non-motor imagery. Furthermore, it allows us to test for non-linear statistics of the data (here the maximum HG power change over the cortical volume and over time) and it is less sensitive to outliers in single

trials, thus ensuring trial-to-trial stability of the average HG power. For the permutation test, which is described in detail in (Pantazis et al. 2005), we randomly exchange a one second interval from (-1s to 0s) of the base line with the signal interval (0s – 1s) for half of all the trials, before computing the average time varying amplitude for a given frequency across trials.

Such a surrogate signal is computed for every voxel in our cortical map. By repeating this step n times, we can build up a histogram for any statistic we wish to compute on the amplitude Z-scores. Since we postulate an increase in HG amplitude in the signal interval, we chose the maximum of the Z-score over the signal period. Since motor imagery is subject initiated, we expect onset times of any HG changes to vary substantially between subjects. By taking the maximum over the signal interval, our statistic is independent of individual variation in that period. Also, for the permutation test, we avoid having to correct resulting p-values of the test for multiple comparisons across e.g. different time points. Non invasive, scalp based approaches (F Darvas et al. 2010; Cheyne et al. 2008; Felix Darvas, Rao, and Murias 2013) have shown that HG activity in the motor system is relatively narrow band and can vary across individuals. Therefore, for the permutation test, we test over the whole band from 70 Hz to 100 Hz in 1 Hz steps and again, choose the maximum Z-score across frequencies. Finally, due to the variant spatial resolution of the inverse mapping, we also select the maximum across all voxels of the map, i.e. the whole cortex. By building a histogram over the maximum in time, frequency and space, we avoid having to correct the resulting p-values for any multiple comparisons. The permutation test also implicitly examines trial-to-trial stability of the average. That is, since any outlier trial with large HG power in the signal interval, which could cause the average HG power to be high as well, has a 50% chance of being permuted with a baseline segment and would skew the baseline HG power distribution in the same manner, the resulting average power would consequently no longer be in the tail end of the baseline distribution. Therefore, increases in the average HG power over trials in the signal period due to outliers will be tested as non-significant

3.2.9 *EMG/EOG Data Processing*

EMG and EOG are sources of noise in the HG band and can exceed the cortical signal considerably. EOG electrodes were placed approximately 1 cm above the left and right brows and 1 cm below left and right eyes. Through the permutation test on the EEG data, we can make sure that any significant HG effects observed in the data are not due to e.g. transient, non-stimulus induced HG activity originating from either EMG or EOG. However, any stimulus-induced, systematic EMG or EOG activity that would introduce an artifact into the EEG would still pass the permutation test. In order to rule out such systematic contamination, we compute the average EMG and EOG HG power over all trials. This was then subsequently entered into into the EEG source analysis to identify systematic increases in HG in the EMG and EOG channels. Since EMG and EOG are typically of broadband nature, in the range from 70-100 Hz, we band pass filtered both signal types for each subject and side and computed the mean amplitude from the Hilbert transform of the 70-100 Hz filtered signals. Because the human brain's power spectrum recorded non-invasively hits the noise floor at around 100 Hz, this 70-100 Hz band pass filter was applied to EEG recordings.

3.2.10 *Determining Goodness of Match Between EEG HG and fMRI and its Significance*

In order to determine how well the HG EEG map and the fMRI match, we group the significant fMRI activity and significant HG activity (i.e. at $p<0.1$) into contiguous clusters on the cortical surface. For each cluster we compute a centroid position and a mean spherical radius, i.e. the mean distance of each cluster member from the center. For each EEG and fMRI cluster, we compute the distance between modalities as the distance between the centroids minus the sphere-radius for each cluster. Negative distances, due to overlap of clusters, are set to zero. For all fMRI clusters, we select the distance to the nearest EEG cluster. If there are more fMRI clusters than EEG clusters, we select smallest distances, matched to the number of EEG clusters.

A compound measure is formed by taking the median across these minimal distances. This will serve as our assessment of the goodness of match between solutions.

Using 3D distances instead of actual geodesic distances on the folded cortical surface is a simplification of the ground truth match between modalities. However, deviations from the 'true' distance are expected to be small, as we expect this value to be dominated by gross mismatches on the order of several centimeters and our measure merely serves as proxy for the goodness of match.

To compute statistical significance for our goodness-of-fit measures, we resampled the fMRI clusters on the cortical surface for each subject and condition (left or right imagery), where we keep the number of clusters and the cluster size constant between our permutation and the original. Thus we can build a histogram of goodness of match values for arbitrary fMRI solutions of similar shape to the original. A p-value, and thus a measure of the specificity of the actual match, is derived by comparing the actual measure vs. the resampled value. We generate 1000 resamples per subject and condition to provide for a sufficient accuracy of the computed p-values.

3.3 RESULTS

3.3.1 *HG EEG Activity*

EEG and fMRI data were collected on separate days in the same group of ten subjects using identical behavioral protocols (see fig. 1 for the EEG montage used). As stated previously in chapter 2, the ***only*** significant task induced EMG activity between 0 and 2000 ms after motor imagery cue onset was found in subject 4 (fig. 2 & 3). There was significant increase in EOG activity in subject 5 after 2000 ms, but also not overlapping with any cortical HG activity (fig. 4 & 5).

The EEG results show significant power increases in the HG band during motor imagery (fig. 6 for subjects 5 and 8. For the remaining 8 subjects, see fig. 7 and fig. 8). These power increases were spatially focal and mostly restricted to the sensorimotor areas of the contralateral cortex, but do cover other cortical areas, not typically associated with motor imagery as well. Single-subject fMRI activity, which is also shown in figures 5-8, also does overlap in most subjects with the EEG reconstruction, but also shows unrelated activity. We find at least one cluster with $p<0.05$ in 9 out 10 subjects for right hand imagery and in 8 out of 10 subjects for left hand imagery. Two subjects had only HG activity with $p<0.1$ for one side (subject 6 for left hand imagery and subject #9 for right hand imagery). Subject #10 had no significant HG activity for left hand imagery.

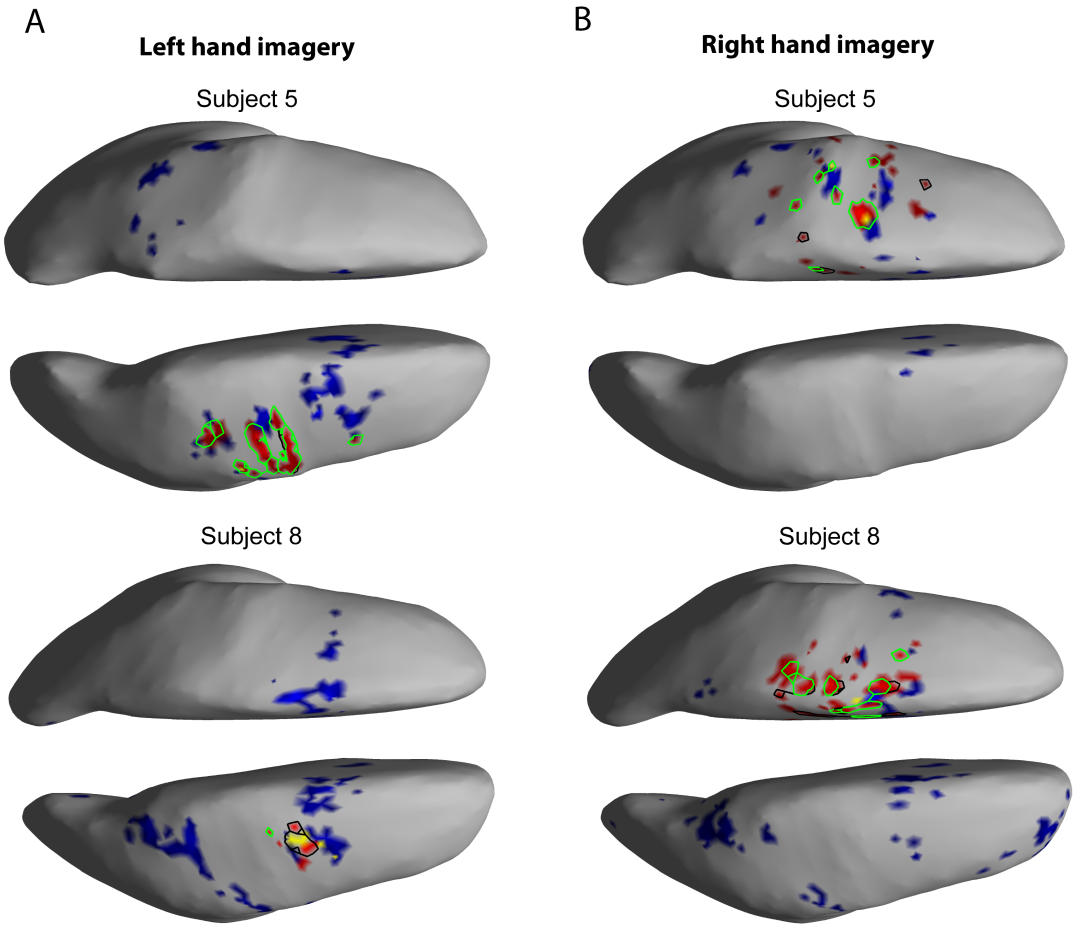

Figure 3.1. EEG and fMRI BOLD activity mapped to realistic cortical headmodels of subjects 5 and 8. The cortical surfaces have been smoothed for better visibility. Blue indicates significant fMRI BOLD activity at Z-score > 2.3. Red indicates significant EEG HG activity at Z >7, the black contour line shows HG at p <= 0.1, the green contour line shows HG at p <= 0.05, and yellow colored areas show overlap between fMRI and EEG. A) Cortical activity during left hand motor imagery. B) Cortical activity during right hand motor imagery.

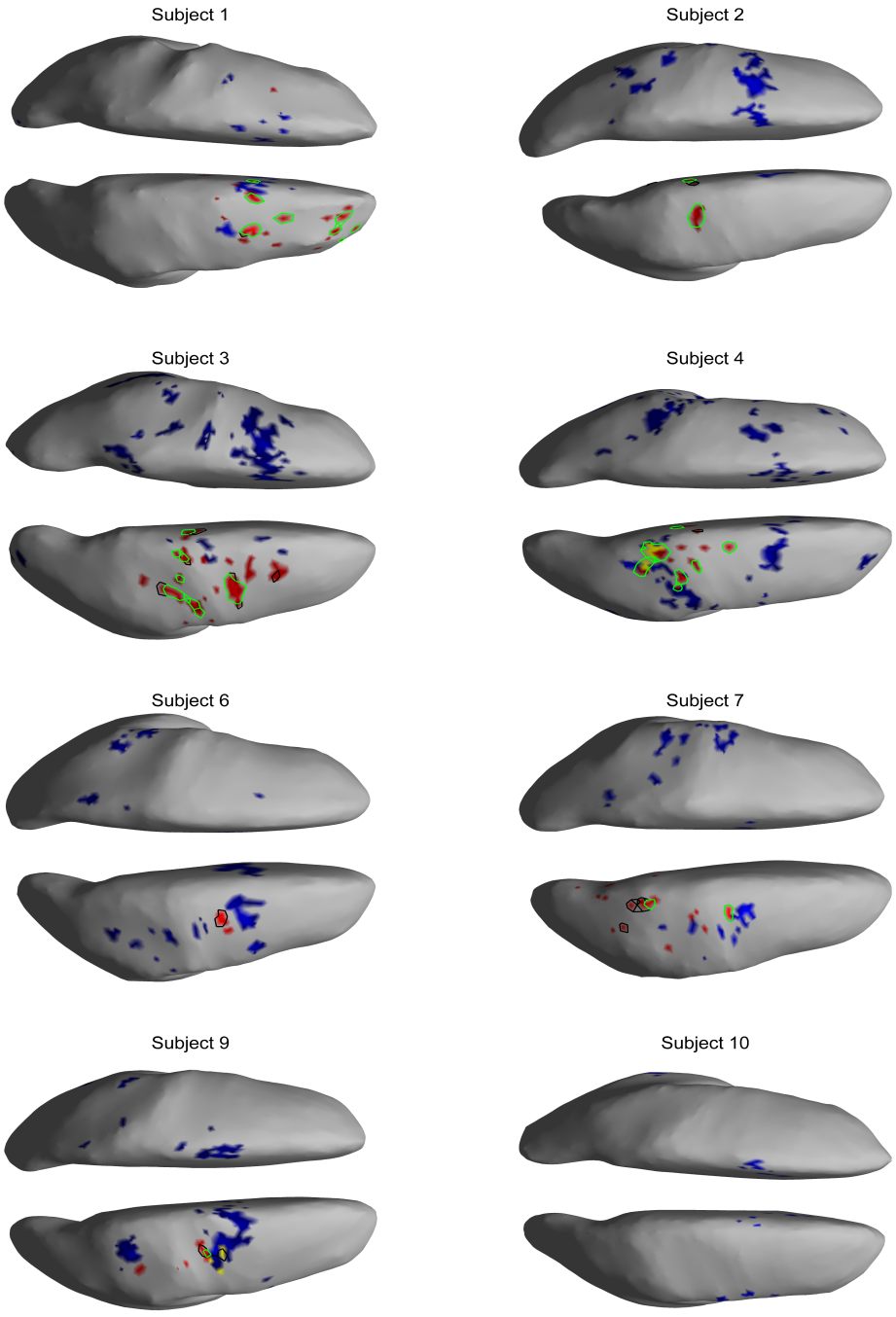

Figure 3.2. EEG and fMRI BOLD activity mapped to realistic cortical headmodels of 7 of the remaining subjects during left hand motor imagery. The cortical surfaces have been smoothed for better visibility. Blue indicates significant fMRI BOLD activity at Z-score > 2.3. Red indicates significant EEG HG activity at Z >7, the black contour line shows HG at p <= 0.1, the green contour line shows HG at p <= 0.05, and yellow colored areas show overlap between fMRI and EEG. A) Cortical activity during left hand motor imagery. B) Cortical activity during right hand motor imagery.

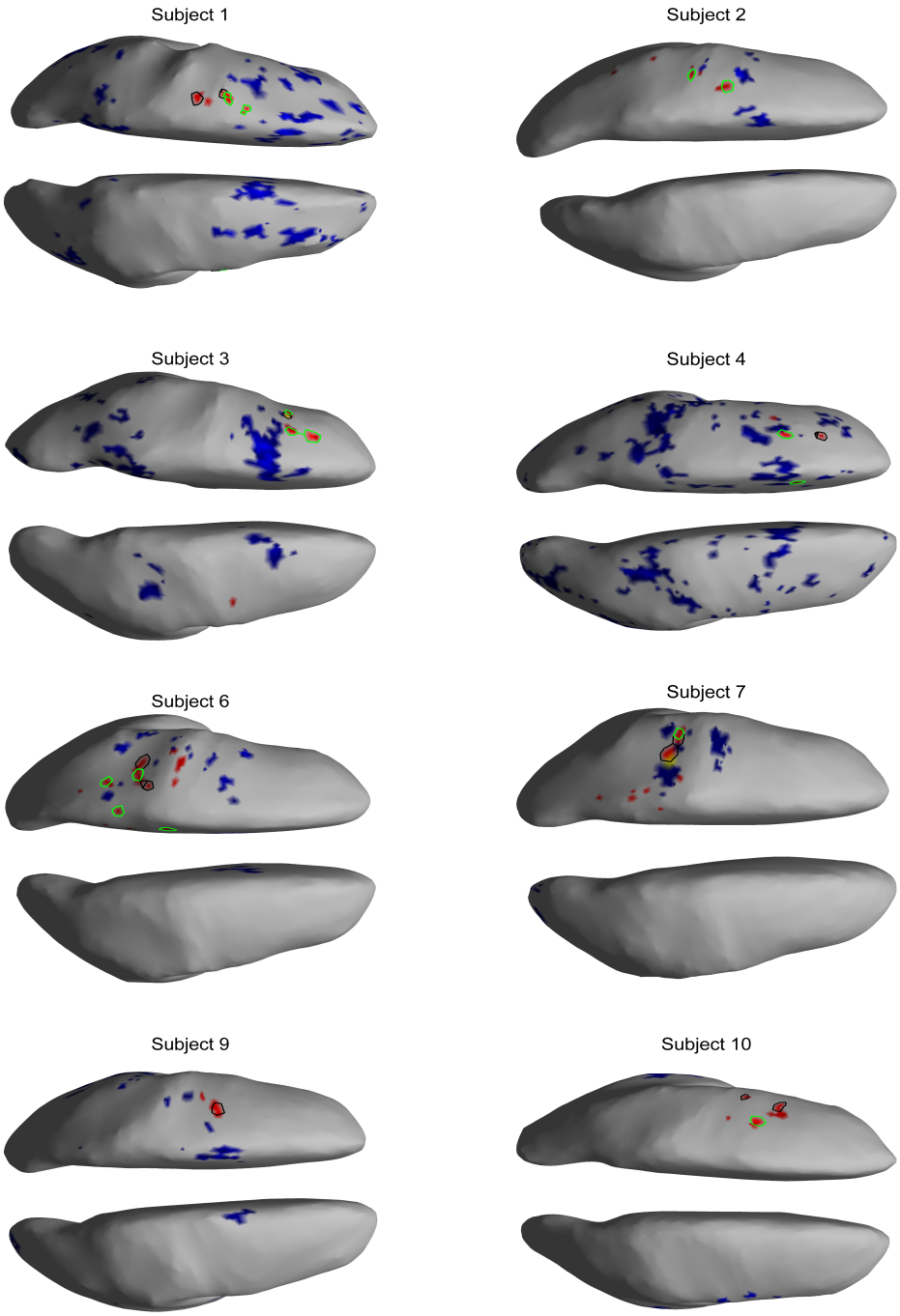

Figure 3.3. EEG and fMRI BOLD activity mapped to realistic cortical headmodels of the 8 remaining subjects during right hand motor imagery. The cortical surfaces have been smoothed for better visibility. Blue indicates significant fMRI BOLD activity at Z-score > 2.3. Red indicates significant EEG HG activity at Z >7, the black contour line shows HG at p <= 0.1, the green contour line shows HG at p <= 0.05, and yellow colored areas show overlap between fMRI and EEG. A) Cortical activity during left hand motor imagery. B) Cortical activity during right hand motor imagery.

3.3.2 *Spatial Correlation Between fMRI BOLD Response and EEG HG Activity*

The task-related fMRI BOLD changes are also shown in Fig. 6 along with the EEG source changes in HG bands on an inflated cortical surface for the imagination of movement of the left and right hands for subjects 5 and 8 (data for the remaining eight subjects are shown in fig. 7 and fig. 8). Individual fMRI results showed BOLD signal increases both in the sensorimotor areas as well as additional BOLD signal increases in the surrounding cortical areas that are varied across subjects. Averages of the fMRI activity during the motor imagery of the left and right hand of all ten subjects are shown in fig. 3.4. Individual fMRI activity spatially co-localizes with the EEG locations of significant power increases in the HG band in most subjects, albeit due to the sometimes more widespread fMRI activity. We find our measure of proximity ranging from 3 to 32 mm (mean 14 mm, 8 mm std.) across all subjects and conditions (except for subject 10, left imagery, where no match exists). P-values range from $p<0.001$ to $p<0.84$, but we find across 7 subjects at least 1 condition with $p<0.05$ and among those 2 with both conditions at $p<0.05$. Distances and p values are listed in table 2. In most cases there is a correlation between small proximity measures and significance, but in cases where there are many fMRI clusters spread out across the cortex, the specificity of the solution remains still small.

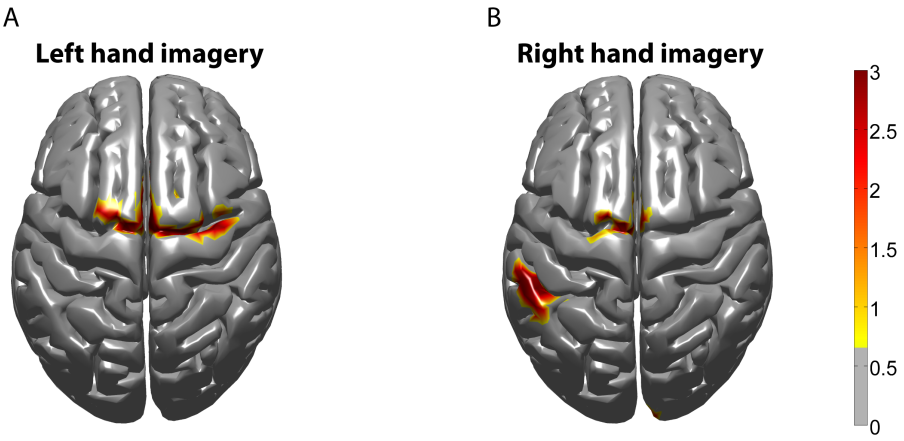

Figure 3.4. Z-score group average fMRI BOLD maps of all subjects (n=10). fMRI BOLD activity was averaged from all subjects in standard Montreal Neurological Institute (MNI) space. A) Averaged fMRI BOLD activity during left hand motor imagery. B) Averaged fMRI BOLD activity during right hand motor imagery. The threshold was determined from a mixed effect model, correcting for multiple comparisons at the group level, using a Gaussian weighted cluster correction at $p < 0.05$.

Table 3.1. Results of the proximity analysis for all 10 subjects and left/right imagery.

Subject	Proximity – left [mm]	*p*-value left	Proximity – right [mm]	*p*-value – right
1	18	0.00	12	0.44
2	27	0.70	15	0.00
3	23	0.58	7	0.19
4	5	0.04	4	0.10
5	3	0.01	12	0.00
6	6	0.04	6	0.00
7	25	0.06	6	0.00
8	15	0.06	19	0.03
9	14	0.33	11	0.66
10	NA	NA	32	0.84

Proximity is the average minimal distance between fMRI clusters and EEG clusters. The p-value is an indication of the specificity of the particular match, computed from a permutation of the proximity measure, where the fMRI clusters are spatially resampled.

3.4 DISCUSSION

In this study, we aimed to recover motor-imagery-related EEG changes in the HG band and examine its spatial overlap with evoked hemodynamic responses. To study this, we collected EEG and fMRI BOLD data of subjects performing a left and right hand motor imagery task in separate sessions. We compared spatial maps of fMRI BOLD signal changes to HG spectral power changes in the measured EEG potential during the motor imagery task. Both modalities were carefully co-registered to allow for direct comparison. Our results show that HG activity during motor imagery can be recovered with EEG using an individual subject's anatomical head model and inverse modeling methods. This high frequency spectral power change has been shown to correlate directly with firing rate (Whittingstall and Logothetis 2009; Manning et al. 2009; K J Miller et al. 2009) and has been demonstrated to reflect broad spectral changes across all frequencies (Kai J Miller et al. 2007; K J Miller et al. 2009). Furthermore, cortical increases in HG band activity recorded with EEG co-localized with an increase of the fMRI BOLD signal.

EEG HG and fMRI co-localization within the motor network

Group averaged beta decreases across the motor system during EEG recordings and increases of the fMRI BOLD signal show spatial co-localization, but individual HG results co-localize best to individual fMRI results and do not produce a coherent grand-average map. This is consistent with ECoG studies that show HG is better than beta frequencies in terms of localization on an individual basis (Hermes et al. 2012). In addition to motor cortex, EEG HG *and* fMRI activity were found in other cortical areas, which did not overlap when subjected to averaging to common brainspace (MNI152). This is different from our earlier work on HG activity during overt movement (F Darvas et al. 2010), where a generic model was used to map HG activity, but more importantly active movement was used and the EEG signal was segmented based on

actual EMG onset. This can be expected to produce a stronger and temporally better aligned HG response than motor imagery, where the only indication of onset of activity is given by the cue.

Since fMRI measures blood oxygenation as a proxy for neuronal activity and the EEG signal is a direct measure of the activity of large groups of coherently active neurons, co-localization of the two modalities is not strictly necessary. Additionally, different layers of neurons in the generation of the two signals are involved (Nunez and Silberstein 2000), which can overlap in activation for a given task, but do not have to.

The scattered nature of the EEG localization, but also of the fMRI activity in our results could be attributable to differences in a subject's imagery strategy. Additionally, any EEG inverse mapping method is prone to localization errors, e.g. the LCMV beamformer that we used, can introduce spurious spatial localizations, even from single "true" sources, where the time series of the reconstructed sources matches the original source, thus leading to a robust result with our trial-to-trial stability test.

Chapter 4. DETECTION OF CORTICAL MOTOR ACTIVITY WITH SUBDERMAL ELECTRODES

4.1 INTRODUCTION AND BACKGROUND

Long-term EEG monitoring is useful for monitoring physiological changes in brain function, such as epileptic seizures, as well as changes in brain signals that can be used to control brain-computer interface (BCI) devices. However, continuous, long-term EEG monitoring is difficult to perform on awake, ambulatory patients due to increased artifacts from muscles and electronic interference. Current surface EEG systems require continuous supervision with frequent electrode readjustments to acquire quality data over extended periods of time (days to months). In addition, common artifacts generated by these recording systems during movement can lead to misleading clinical diagnosis and suboptimal control signals for BCI systems. An implanted, stable, subdermal electrode system could provide the high fidelity signals necessary for the long-term control of a BCI device.

Prior research has shown that subdermal wire electrodes maintain good recording characteristics with stable impedances for long-term monitoring of EEG signals (Martz, Hucek, and Quigg 2009). In addition, subdermal wire electrodes have been found to be less susceptible to artifacts than surface electrodes (Young et al. 2006). A study comparing the alpha attenuation over the occipital lobe during eye closure in an implanted subcutaneous system to a surface EEG system found the recordings of both systems to be similar (Duun-Henriksen et al. 2015). The investigators also concluded that the subcutaneous recording system provides a stable signal with long-term use (26 days).

Research comparing subgaleal and ECoG recordings have shown that neural signals outside of the skull are attenuated linearly and can be recorded up to 110 Hz (Olson et al. 2015). Their study indicated that subgaleal electrodes could record HG signals without frequency distortion

from the skull. In addition, Olson and colleagues (Olson, Wander, and Darvas, unpublished.) have reported activity dependent changes in beta and HG frequency bands recorded with subdermal electrodes during the same finger tapping task outlined in this chapter. They observed decreases in the beta frequency band power (Figures 4.1 and 4.2) over motor areas of the cortex that preceded and coincided with movement. In addition, they were able to spatially localize high gamma activity that preceded movement by implementing a spatial beamformer over all subjects to increase the SNR of the HG band (Figure 4.3).

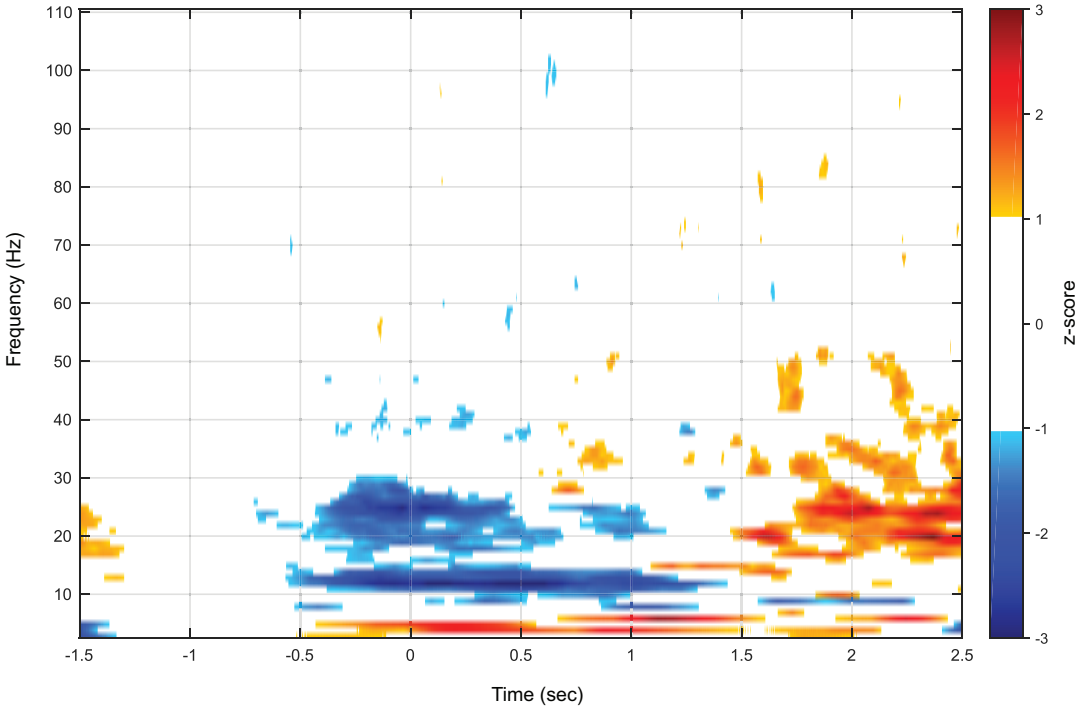

Figure 4.1: Median spectrogram across all bipolar channels and subjects. Adopted from Olson, Wander, and Darvas. Not published. The median was used to make the presentation more robust to outliers, which e.g. can be clearly seen in figure 3. The median spectrogram has been normalized using the z-transform with a baseline period from -1.5 s to -0.7s before movement onset. Blue represents decrease in power relative to baseline, red an increase. Z-scores between -1 and 1 have been masked for better visual clarity. The time axis ranges from -1.5 s prior to EMG onset to 2.5 s post EMG, the frequency axis covers a range from 3 to 100 Hz. There is a clear movement induced alpha/beta suppression and beta rebound visible across the area surveyed with the needle electrodes, well in line with the literature on non-invasive EEG recording of movement over motor areas.

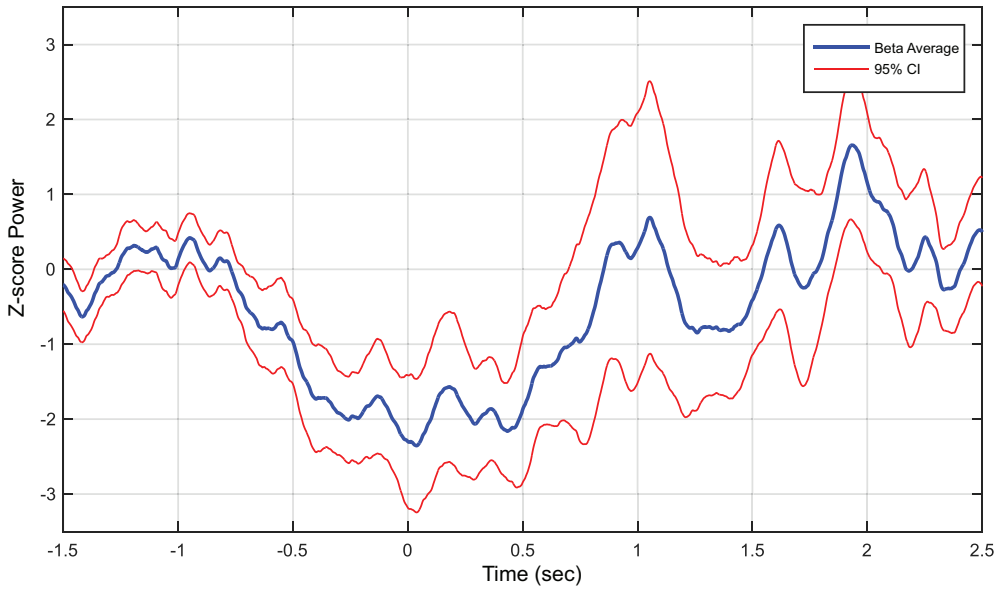

Figure 4.2: Average beta power across all subjects and electrodes from a band pass filter (17-25 Hz). Adapted from Olson, Wander, and Darvas. Not published. Blue show the z-transformed beta power averaged across all monopolar channels and subjects. Red shows the 95% CI across subjects. Like figure 5, this shows the typical beta power behavior for voluntary movements: initial depression, followed by a later rebound.

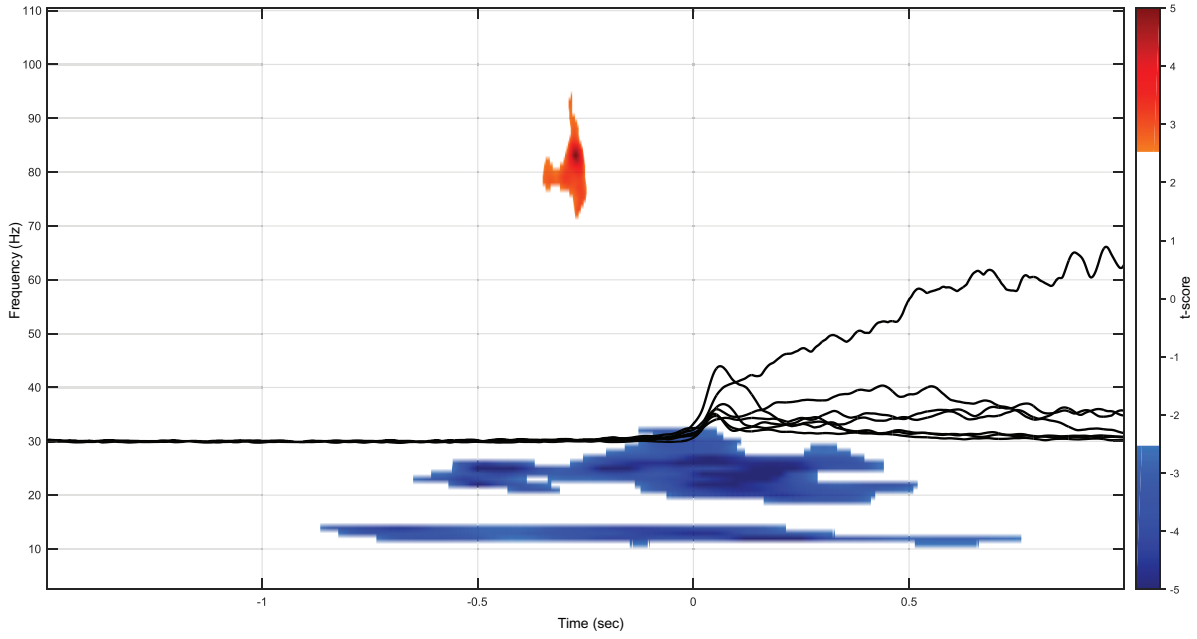

Figure 4.3: T-statistic of the comparison between beamformed resting period spectrograms and voluntary movement spectrograms, subjected to a cluster-correction across all subjects. Adapted from Olson, Wander, and Darvas. Not published. Clusters shown are globally significant, across all subjects, at $p<0.05$. Red indicates significant increase in power vs. rest, blue significant decrease. The black lines show individual EMG traces for each subject. There is significant HG power increase prior to EMG onset, with a relative timing to the beta decrease similar to previous non-invasive studies (Darvas et. al. 2009, High gamma mapping in EEG).

The aim of this study was to investigate the motor related brain activity of healthy subjects in the mu, beta, and high gamma frequency bands recorded using subdermal EEG electrodes. Cortical activity was recorded over the motor regions of the cortex while healthy subjects participated in a finger-tapping task. To assess the quality of these subdermal recordings they were compared to recordings performed simultaneously using surface EEG electrodes. This study found neural recordings using subdermal electrodes were comparable to those of surface recordings, and thus these subdermally detected motor-related brain signals may prove to be used for the development of BCIs that can be used reliably for long-term outpatient use.

Results of the following work are to be published in:

Smith, M.M., Olson, J.D., Rao, R.P.N., Darvas, F., "Utilizing Subdermal Electrodes as a Non-invasive Alternative for Motor-based BCIs". Brain Computer Interfaces Handbook: Technological and Theoretical Advances.

4.2 MATERIALS AND METHODS

4.2.1 *Subjects*

Data were recorded from healthy subjects that provided their informed consent according to the protocol approved by the Institutional Review Board (IRB) at the University of Washington.

4.2.2 *Electrodes and Electrode Placement*

To detect movement onset, surface electromyography (EMG) electrodes were placed over the forearm flexor with reference and ground electrodes placed on bony prominences at the wrist to minimize electrocardiogram (ECG) artifacts.

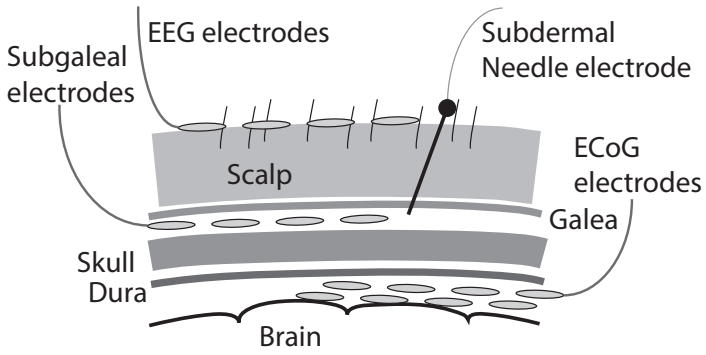

Figure 4.4. Schematic of subdermal needle electrode depths relative to other common recording locations and relevant layers of anatomy. Not to scale. *Adapted from Olson et al. 2015.*

Using clean technique, bare-metal FDA approved subdermal needle electrodes (Rochester Electro-Medical, Lutz, FL) were placed at the bone-scalp interface depicted in Figure 1, with 2 electrodes around C3/C4, 1 reference at Cz, and 1 ground at G using the standard scalp EEG 10-20 system (Niedermeyer and Lopes da Silva 2004) as in Figure 2. Surface electrodes were placed directly above subcutaneous electrodes. Subcutaneous electrodes were placed directly under the surface electrodes. Electrode pairs were placed approximately one inch apart from each other.

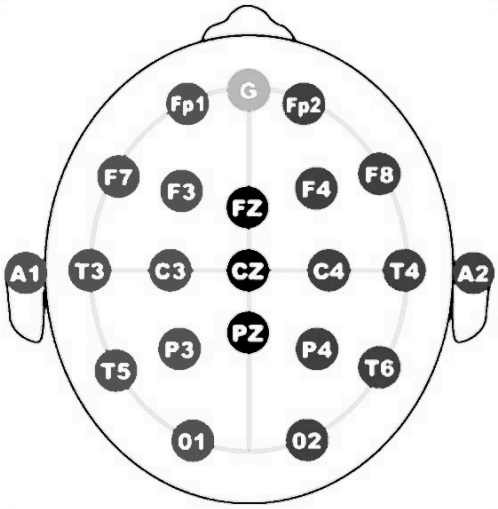

Figure 4.5. Location of needle electrodes relative to the accepted 10-20 EEG system. Electrodes were placed around C3/C4, with 1 reference at Cz, and 1 ground at G.

4.2.3 *Task*

Subjects were cued to move either their left or right forefinger once per trial. Subjects were seated in a recliner and four blocks of 25 right and 25 left hand trials were recorded (only left hand trials were recorded and executed from Subject 2), totaling 100 trials per hand. The subjects had their eyes open and fixated on a cross or cue. Each trial consisted of a rest period of 2 seconds, during which a fixation cross was shown. At the end of that rest period the fixation cross was changed to a written instruction, which indicated either "right" for right finger movement, or "left" for left finger movement. The cue was shown for 3 seconds and then changed back to a fixation cross, which concluded the trial. During each block "left" and "right" cues were presented in random order, for a total of 50 cues per block.

4.2.4 *Data Acquisition*

Surface and subdermal EEG data were continuously recorded during each block. Data were sampled at 1200 Hz using two GugerTec (GugerTec, Graz, Austria) EEG amplifiers recorded in DC from -250 to +250 mV. Impedance values were below 20kΩ for all subdermal and surface electrodes. In parallel, EMG activity was recorded at the same sampling rate from the flexor indices from both hands. Data was high pass filtered at 2 Hz using an 8^{th} order Butterworth filter, as well as notch filtered from 58 to 62 Hz using a 4^{th} order Butterworth filter to remove any line noise.

4.2.5 *Data Preprocessing*

Trials were inspected for artifacts (excessive EMG, eye blinks, etc.) and rejected if any channels showed artifact contamination. Both surface and subdermal EEG data were re-referenced to a common average reference to eliminate any common noise introduced by activity recorded at the reference electrode. Data were then segmented from continuously recorded EEG data into 5

second long segments for each block, with time 0 seconds centered at the onset of movement (detected by EMG) resulting in a within-trial axis ranging from -2 to 3 seconds (rest being between -2 and 0 s).

4.2.6 *Comparing Mu, Beta, and High Gamma Band Power Changes in Subdermal and Surface Electrode Recordings*

In order to compare the strength of the signals recorded with subdermal vs. surface electrodes, power spectra were generated using a windowed FFT. Specifically, a hanning window was applied to each trial, an FFT and squared absolute value were then computed. These results were then averaged over all trials. Data were divided into rest (-1.5 to -0.5 s) and movement (0 to 1 s) periods. The spectra were normalized by dividing by the mean power across all trials at each frequency and the log of the values were determined. To determine the degree of separation in the low frequency (8-30 Hz) and high frequency (70-100 Hz) band powers between rest and movement tasks, the area between the curves in each corresponding frequency range was calculated.

4.2.7 *Comparing Magnitude Squared Coherence Between Subdermal and Surface Electrode Recordings*

To determine the similarity between subdermal and surface electrode recordings, the magnitude squared coherence spectrum was calculated for movement states. The coherence spectrum was computed using Welch's averaged periodogram method (a function of the power spectral densities $P_{xx}(f)$, $P_{yy}(f)$, and the cross power spectral density, $P_{xy}(f)$):

$$C_{xy}(f) = \frac{|P_{xy}(f)|^2}{P_{xx}(f) \,.\, P_{yy}(f)}\,.$$

4.3 RESULTS

4.3.1 *Comparison of Low and High Frequency Band Power Changes in Subdermal and Surface Electrode Recordings*

We found that the power spectra of subdermal electrodes provide similar signals to those of surface electrodes. Current motor-based BCIs typically rely on the change in spectral power in the low or high frequency ranges and in order to assess the degree of differentiation of the change in spectral band powers during a movement task, power spectra during rest and movement periods were compared. Two frequency bands were considered: the low frequency band (8-30 Hz) and high frequency band (70-100 Hz). Figures 1-4 show that the subcutaneous electrodes provide similar differentiation between rest and movement periods, in each of the designated frequency bands, when compared to surface electrodes recorded simultaneously. Table 1 shows a comparison between the areas between the movement and rest power spectra.

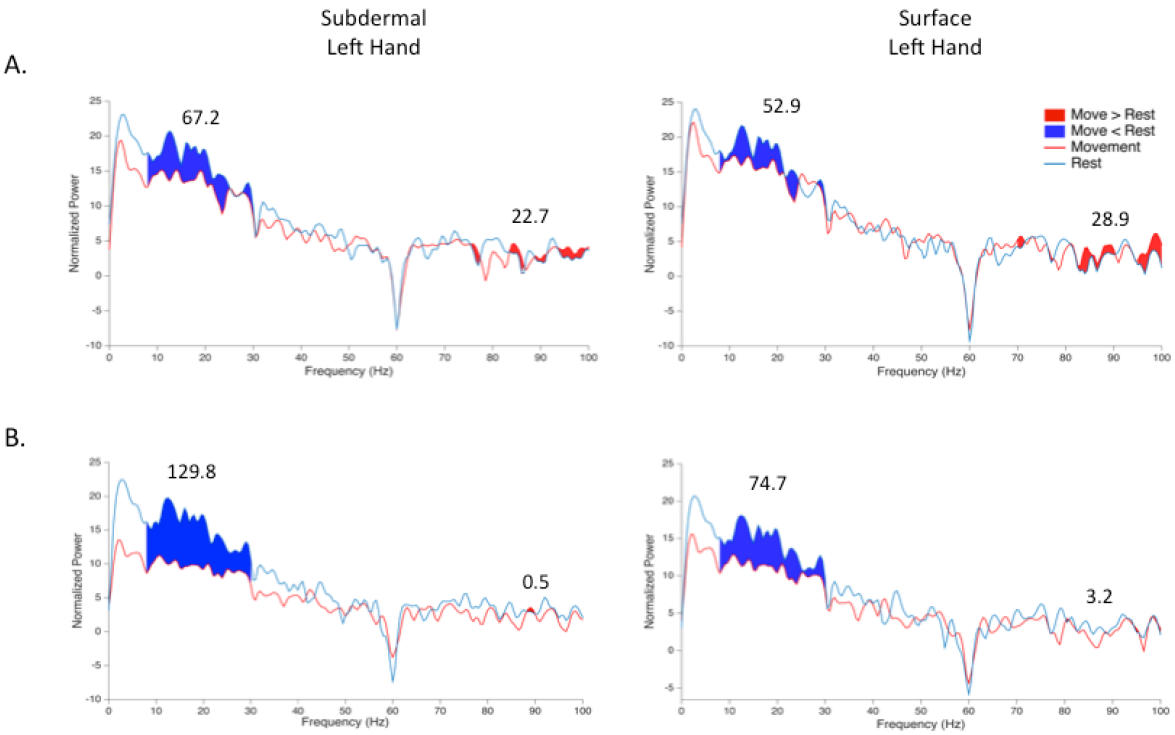

Figure 4.6. A comparison of power spectral densities for subdermal and surface recordings during rest and left hand movement periods recorded from electrode pairs 2 (A) and 4 (B). Spectra are for recordings over C4. Blue power spectra are representative of the normalized power over frequencies 3-100 Hz during the rest period (-1.5 to -0.5 s before movement onset). Red power spectra are representative of the normalized power over the same frequency range during the movement period (0 to 1 s, with 0 s being the onset of movement). Blue fill between rest and movement power spectra represents the area between the two curves in the low frequency band of 8-30 Hz. Red fill between rest and movement power spectra represents the area between the two curves in the high frequency band of 70-100 Hz. Numerical values above each of the low and high frequency bands indicate the value of the area between the two curves in each frequency range.

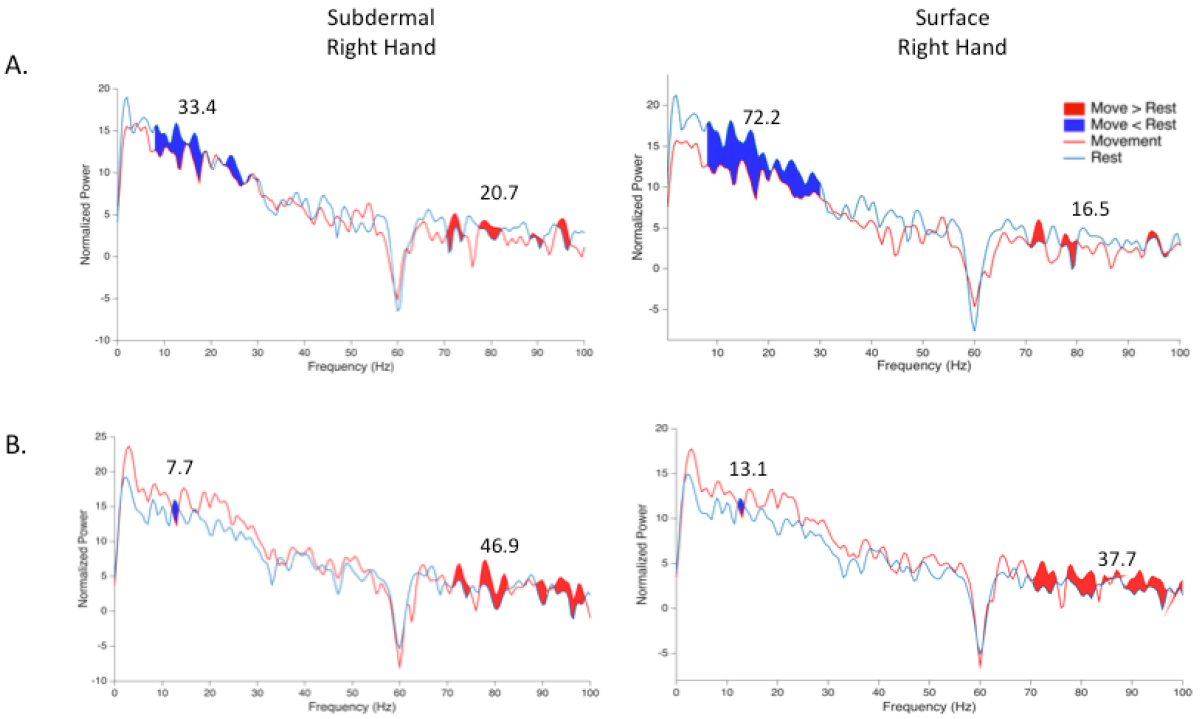

Figure 4.7. A comparison of power spectral densities for subdermal and surface recordings during rest and right hand movement periods recorded from electrode pairs 1 (A) and 3 (B). Spectra are for recordings over C4. Blue power spectra are representative of the normalized power over frequencies 3-100 Hz during the rest period (-1.5 to -0.5 s before movement onset). Red power spectra are representative of the normalized power over the same frequency range during the movement period (0 to 1 s, with 0 s being the onset of movement). Blue fill between rest and movement power spectra represents the area between the two curves in the low frequency band of 8-30 Hz. Red fill between rest and movement power spectra represents the area between the two curves in the high frequency band of 70-100 Hz. Numerical values above each of the low and high frequency bands indicate the value of the area between the two curves in each frequency range.

Table 4.1. Area between movement and rest power spectra in low (8-32 Hz) and high (70-100 Hz) frequency bands. For each subject electrode pair, in each frequency band, the electrode that provides the larger area between the power spectra is given in bold.

Location/Pair #	Low Frequency (8-32 Hz)		High Frequency (70-100 Hz)	
	Subdermal	Surface	Subdermal	Surface
C3/1	33.4	**72.2**	**20.7**	16.5
C3/2	7.7	**13.1**	**46.9**	37.7
C4/3	**67.2**	52.9	22.7	**29.0**
C4/4	**129.8**	74.7	0.5	**3.2**

4.3.2 *Comparison of Magdnitude Squared Coherence Between Subdermal and Surface Electrode Recordings*

To assess the similarities between the signals recorded from subdermal and surface electrodes, the magnitude squared coherence spectrum between each electrode pair was computed. The coherence spectrums in figures 1-4 show that the lower frequencies (< 30 Hz) in each electrode pair have greater coherence than the higher frequencies (2-30 Hz). These coherence results indicate that there appears to be mutual information between the subdermal and surface electrode signals in the low frequency signals, but many of signals in the higher frequencies may be unique to each surface and subdermal electrode.

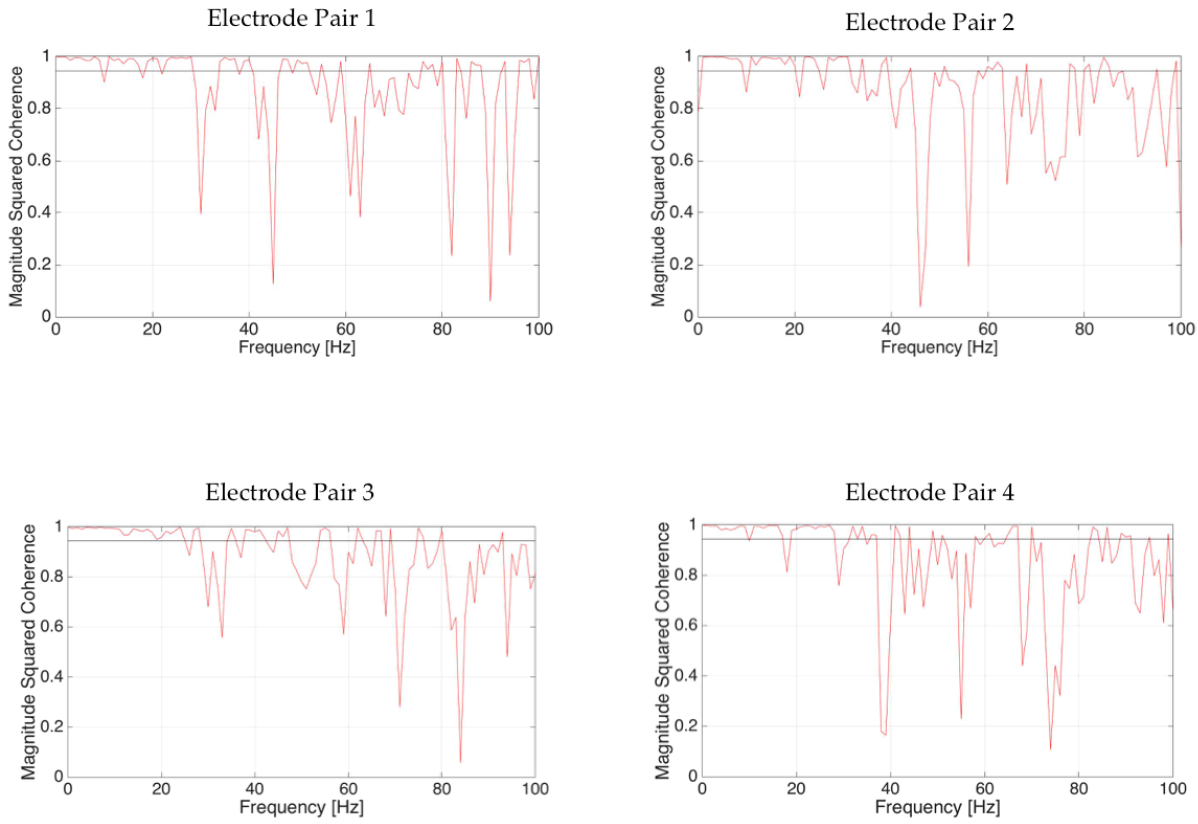

Figure 4.8. Magnitude squared coherence spectrum of electrode pairs 1-4 over C3 during right hand movements and C4 during left hand movements. Black line indicates 95% confidence interval.

4.4 DISCUSSION

The goal of this study was to characterize the movement related cortical signals recorded over the motor cortex using subdermal EEG electrodes. Brain signals were recorded over the contralateral motor cortex while healthy subjects performed a finger-tapping task. Our analysis focused on frequency bands that are frequently used for motor related BCI control signals (mu, beta, and high gamma). Overall, the signals recorded using subdermal needle electrodes were found to be comparable to those recorded simultaneously with surface EEG electrodes.

The spectral and coherence analyses showed that subdermal and surface recording electrodes provide very similar signals, especially in the low frequency bands. Considering that the degree of separation between the power in the low frequency bands during rest and movement in subdermal recordings are similar to those of surface recordings, these results further support the idea that an implantable subdermal electrode system may be able to provide reliable, long-term motor control signals for BCI control.

Several limitations of this study should be noted. The first limitation being that sources of noise could have been introduced due to the instability of the electrode connections to the skin or from induced currents due to movement of the electrodes. These sources of noise may be reduced and the SNR of the system could be improved if the subdermal electrodes are fully implanted with a rigid connection. Second, because high gamma band activity is spatially focal on the cortex compared to the beta band activity it is possible that our single electrode placements could have missed the cortical location of high gamma band activity. Using a high-density electrode array could potentially improve the SNR in the high-gamma band. Third, in order to determine the usefulness of subdermally driven BCI, real-time control of a BCI using these motor-related signals needs to be studied. Lastly, In order to provide reliable, long-term monitoring and BCI control the subdermal recording devise must provide a high SNR with little data loss with long-term use. An extension of this work could assess the fidelity of the signals in longitudinal studies.

Chapter 5. CONCLUDING REMARKS AND FUTURE DIRECTIONS

Over the last few decades, there have been remarkable advances in non-invasive BCIs. Their usability, information transfer, and robustness have been improved, with machine learning and signal processing techniques. BCIs that utilize control signals based on motor imagery have not only proven to be useful for users with limited motor disabilities, but have also shown to facilitate improved motor function during stroke rehabilitation (Ang et al. 2011; Daly et al. 2009; Ramos-Murguialday et al. 2013; Broetz et al. 2010; Prasad et al. 2010). As previously stated, typical non-invasive motor imagery based BCIs rely on ERS/ERD using bandpower in the mu and beta rhythms. Non-invasive recording of the modulation of HG is still a relatively novel concept and most HG studies have been limited to invasive electrocorticography methods, due to the low SNR of the neuronal ensemble activity at these frequencies. Consequently the systematic study of HG effects has been limited to narrow populations (typically epilepsy patients) and cortical locations, which are usually determined by clinical needs rather than by the experimental paradigm one wishes to study. The main strategy of this thesis was to recover HG activity in motor cortex from non-invasive, scalp EEG data during motor imagery. This is a particularly compelling application, as motor imagery presumably generates weaker HG activity than overt motor actions (K. Miller et al. 2010). At the same time, imagery (rather than overt movements) reduces possible confusion or confound with EMG interference in this frequency band. This work serves as proof-of-concept that HG can be studied non-invasively, thus opening up this band to a much wider subject population and range of experimental paradigms.

In addition, the second portion of this thesis presents for the first time a comparison between HG range activity measured non-invasively with EEG and the BOLD response, measured with fMRI, for this same motor imagery paradigm. While the degree of direct overlap between the cortical locations of HG activity detected with EEG electrodes and the spatial distributions of

the fMRI BOLD response in each individual subject was relatively small, our proximity analysis showed the HG and BOLD responses to be in close proximity to each other. There are several possible explanations for the limited amount of direct spatial overlap between the two modalities on the cortex. First, previous studies that have shown a correlation between HG activity and fMRI BOLD activity (Hermes et al. 2012) were performed using ECoG electrodes placed directly on the surface of the brain and significant HG activity was determined for each electrode location. Whereas, our study used inverse modeling techniques to localize significant HG activity on the cortical surface. While HG activity was localized to expected sensorimotor regions of the cortex several factors could have contributed to slight errors in the true location of the source. Errors in detecting boundaries between tissue types when developing our realistic forward head models, conductivity values for each of the tissue layers, and electrode positions can all contribute to source localization errors between 4- 20mm (Akalin Acar and Makeig 2013). Second, Hermes and colleagues were able to minimize fMRI artifacts from the large arterial and venous blood vessels to focus on the BOLD effects originating from the capillary bed using an fMRI acquisition technique; a technique not used for our study. Third, EEG and fMRI recording sessions were performed on different days and each subject may have shifted their motor imagery strategy between recording sessions that could have resulted in altered cortical activation.

When performing inverse modeling techniques for HG source localization, we incorporated estimates, obtained from MRI, of the boundaries between tissues with different conductivity, specifically the cortex, skull, and scalp, into boundary element models. However, because of our limited knowledge of the true conductivities of these tissues it is not clear that these subject specific models represent a significant improvement in source localization over generic head models. An extension of the work presented in this thesis could include a comparison between the strength of the HG signal recovered from a generic head model and the HG signal recovered from an individual's realistic head model.

High gamma signals measured from scalp EEG electrodes are of low amplitude and SNR, especially during motor imagery. Thus, in order to extract relevant high gamma activity during motor imagery we needed to average over many trials (between 50-100 trials) for each subject. These trials were averaged after trials that contained artifacts were rejected, resulting in the loss of potentially useful data and leading to the inability to use the HG signals for real-time BCI control. Empirical mode decomposition (EMD) filtering methods (Huang et al. 1998) have been proposed to correct muscle artifacts in EEG recordings in the time-domain without the need to reject potentially useful data (Chen et al. 2010). One possible extension of our studies is to utilize real-time EMD based filtering techniques to correct for artifacts in the EEG recordings in order to obtain a higher SNR and possible real-time BCI control using the high gamma frequency band.

Future experiments that could build off of the work presented in this thesis include identifying additional cortical areas in non-primary motor regions (such as prefrontal regions) that are activated during voluntary movement, movement observation, or motor imagery. One limitation of current motor imagery-based BCI control methods is that the cortical areas involved are limited to the left and right hand, foot, and tongue regions of the primary motor cortex. Real-time measures of the synchronization/interaction between the non-primary motor cortical areas can be used to enhance specificity of the motor activity and thus facilitate real-time detection. Because the execution of motor or cognitive tasks requires the interaction between multiple cortical regions that exchange their information, incorporating signals that occur outside of the motor cortex to drive a BCI will have significant impact on people with limited motor cortical activity and muscle control, as well as support a BCI with a more flexible range of output.

Additional experiments are prompted by the observation that ECoG signals for a given function (such as finger flexion) differ depending on the task's context, such as pinching the thumb and

forefinger together versus making a fist. These cortical signals are also evident outside of the motor cortex. Thus, it may be possible to decode movement context using information in primary motor or secondary motor areas such as the supplementary motor area. By utilizing the information provided with fMRI it may be possible to identify locations where a specific activity pattern can decode motor context or intention among movements such as 1) simple, self-paced index finger flexion, 2) a pinch task involving repetitive approximation of the tips of the thumb and index finger, 3) fist-formation repeated over the interval, and 4) tactile exploration of objects. After localizing these context specific regions, we can then attempt to use them to support a BCI that will distinguish what hand movements are being imagined by the subject. These spatially distinct signals may be used for multiple control signals for the dynamic control of a BCI devise.

The third portion of this thesis was based on the knowledge that electrodes placed closer to the brain provide greater signal than those that are placed further away on top of the scalp. As a general rule, the amplitude of recorded brain signals decreases proportionally to the inverse square of the distance from the source. Therefore, ECoG electrodes provide a signal that is many degrees of magnitude larger than the signal recorded from surface EEG electrodes. However, ECoG electrodes are considered invasive, as they require surgery to place the electrodes on the surface of the brain. Subdermal electrodes placed below the scalp may provide an intermediate option in regards to the degree of invasiveness and signal quality when compared to surface EEG electrodes. Several studies have shown that subdermal electrodes enhance the precision and accuracy of EEG measurements compared to scalp EEG electrodes (Wendel et al. 2010; Subramaniyam et al. 2011). The data analysis outlined in this thesis was intended to determine the capacity to record brain signals with subdermal electrodes, focusing on characterizing the movement related cortical signals that are relevant to BCI research recorded over the motor cortex. Our results show that the motor-related signals recorded with subdermal electrodes are comparable to scalp EEG electrodes. While the intent of the data

analysis did not include a comparison of the SNR between subdermal and scalp EEG electrodes, our results, in conjunction with previous studies showing an improved SNR in subdermal electrodes when compared to scalp EEG eelctrodes (Subramaniyam et al. 2011; Wendel et al. 2010), show that subdermal electrodes may provide an intermediate option between scalp and ECoG electrodes when studying motor-related brain signals. While invasive recordings such as ECoG still provide a greater SNR than subdermal electrodes, it is possible that the SNR of the subdermal system could be improved if the subdermal electrodes were fully implanted with a rigid connection. In addition, a fully implanted subcutaneous system with wireless telemetry could provide a long-term option for a BCI device or clinical monitoring.

The major contributions of this work include the ability to non-invasively detect and localize high gamma activity on the cortex during a motor-imagery task. While this high gamma activity has the potential to provide a faster, more responsive BCI control signal than signals currently used for non-invasive BCIs, more advanced algorithms need to be developed and applied in order to be able to utilize this high gamma band in real-time non-invasively. In addition to refined algorithms, electrodes that are optimally placed could improve high gamma signal quality. Placing an implanted subdermal electrode system in optimal locations under the scalp could provide the high fidelity signals necessary for the long-term control of a motor-related BCI device. Taken together, the work outlined in this thesis suggests that a subdermally implanted BCI system that utilizes beam-formed HG control signals in real-time could provide a long-term, fast-response, non-invasive BCI option.

REFERENCES

Ahi, Sercan Taha, Student Member, Hiroyuki Kambara, and Yasuharu Koike. 2011. "A Dictionary-Driven P300 Speller" 19 (1): 6–14.

Akalin Acar, Zeynep, and Scott Makeig. 2013. "Effects of Forward Model Errors on EEG Source Localization." *Brain Topography* 26 (3): 378–96..

Andersen, Richard, Lawrence Snyder, David Bradley, and Jing Xing. 1997. "Multimodal Representation of Space in the Posterior Parietal Cortex and Its Use in Planning Movements." *Annual Review of Neuroscience* 20: 303–30. doi:10.1146/annurev.neuro.20.1.303.

Ang, Kai Keng, Cuntai Guan, Karen Sui Geok Chua, Beng Ti Ang, Christopher Kuah, Chuanchu Wang, Kok Soon Phua, Zheng Yang Chin, and Haihong Zhang. 2011. "A Large Clinical Study on the Ability of Stroke Patients to Use an EEG-Based Motor Imagery Brain-Computer Interface." *Clinical EEG and Neuroscience* 42 (4): 253–58.

Bai, Ou, Peter Lin, Sherry Vorbach, Mary Kay Floeter, Noriaki Hattori, and Mark Hallett. 2008. "A High Performance Sensorimotor Beta Rhythm-Based Brain-Computer Interface Associated with Human Natural Motor Behavior." *Journal of Neural Engineering* 5 (1): 24–35..

Baizer, J S, L G Ungerleider, and R Desimone. 1991. "Organization of Visual Inputs to the Inferior Temporal and Posterior Parietal Cortex in Macaques." *The Journal of Neuroscience : The Official Journal of the Society for Neuroscience* 11 (1): 168–90.

Ball, T, E Demandt, I Mutschler, E Neitzel, C Mehring, K Vogt, A Aertsen, and A Schulze-Bonhage. 2008. "Movement Related Activity in the High Gamma Range of the Human EEG." *NeuroImage* 41 (2): 302–10. doi:DOI 10.1016/j.neuroimage.2008.02.032.

Bar, M, K S Kassam, a S Ghuman, J Boshyan, a M Schmid, a M Schmidt, a M Dale, et al. 2006. "Top-down Facilitation of Visual Recognition." *Proceedings of the National Academy of Sciences of the United States of America* 103 (2): 449–54.

Basar-Eroglu, C, C Schmiedt-Fehr, and B Mathes. 2012. "Auditory Evoked Alpha Osillations Imply Reduced Anterior and Increased Posterior Amplitudes in Schizophrenia." *Clin Neurophysiol* 62: 121–29.

Başar, E, B Güntekin, I Atagün, B Turp Gölbaşı, E Tülay, and a Ozerdem. 2012. "Brain's Alpha Activity Is Highly Reduced in Euthymic Bipolar Disorder Patients." *Cognitive Neurodynamics* 6 (1): 11–20.

Belitski, a, J Farquhar, and P Desain. 2011. "P300 Audio-Visual Speller." *Journal of Neural Engineering* 8 (2): 25022.

Blatt, GJ, RA Andersen, and GR Stoner. 1990. "Visual Receptive Field Organization and Cortico-Cortical Connections of the Lateral Intraparietal Area (Area LIP) in the Macaque." *J Comp Neurol* 299 (4): 421–45.

Broetz, Doris, Christoph Braun, Cornelia Weber, Surjo R Soekadar, Andrea Caria, and Niels Birbaumer. 2010. "Combination of Brain-Computer Interface Training and Goal-Directed

Physical Therapy in Chronic Stroke: A Case Report." *Neurorehabilitation and Neural Repair* 24 (7): 674–79.

Buch, Ethan, Cornelia Weber, Leonardo G Cohen, Christoph Braun, Michael a Dimyan, Tyler Ard, Jurgen Mellinger, et al. 2008. "Think to Move: A Neuromagnetic Brain-Computer Interface (BCI) System for Chronic Stroke." *Stroke; a Journal of Cerebral Circulation* 39 (3): 910–17.

Bullier, J. 2001. "Integrated Model of Visual Processing." *Brain Research. Brain Research Reviews* 36 (2-3): 96–107.

Bundy, David T, Mark Wronkiewicz, Mohit Sharma, Daniel W Moran, Maurizio Corbetta, and Eric C Leuthardt. 2012. "Using Ipsilateral Motor Signals in the Unaffected Cerebral Hemisphere as a Signal Platform for Brain-Computer Interfaces in Hemiplegic Stroke Survivors." *Journal of Neural Engineering* 9 (3): 036011.

Buzsáki, György, Costas a Anastassiou, and Christof Koch. 2012. "The Origin of Extracellular Fields and Currents--EEG, ECoG, LFP and Spikes." *Nature Reviews. Neuroscience* 13 (6). Nature Publishing Group: 407–20.

Chen, D, D Li, M Xiong, H Bao, and X Li. 2010. "GPGPU-Aided Ensemble Empirical-Mode Decompositin for EEG Analysis During Anesthesia." *IEEE Transactions on Information Technology In Biomedicine* 14 (6).

Cheyne, Douglas, Sonya Bells, Paul Ferrari, William Gaetz, and Andreea C Bostan. 2008. "Self-Paced Movements Induce High-Frequency Gamma Oscillations in Primary Motor Cortex." *NeuroImage* 42 (1): 332–42.

Conner, Christopher R, Timothy M Ellmore, Thomas A Pieters, Michael A DiSano, and Nitin Tandon. 2011. "Variability of the Relationship between Electrophysiology and BOLD-fMRI across Cortical Regions in Humans." *The Journal of Neuroscience* 31 (36): 12855–65.

Crammond, D J, and J F Kalaska. 2000. "Prior Information in Motor and Premotor Cortex: Activity during the Delay Period and Effect on Pre-Movement Activity." *Journal of Neurophysiology* 84 (2): 986–1005.

Crone, N E, D L Miglioretti, B Gordon, and R P Lesser. 1998. "Functional Mapping of Human Sensorimotor Cortex with Electrocorticographic Spectral Analysis. II. Event-Related Synchronization in the Gamma Band." *Brain : A Journal of Neurology* 121 (Pt 1 (December): 2301–15.

Dalal, S S, A G Guggisberg, E Edwards, K Sekihara, A M Findlay, R T Canolty, M S Berger, et al. 2008. "Five-Dimensional Neuroimaging: Localization of the Time-Frequency Dynamics of Cortical Activity." *NeuroImage* 40 (4): 1686–1700.

Daly, Janis J, Roger Cheng, Jean Rogers, Krisanne Litinas, Kenneth Hrovat, and Mark Dohring. 2009. "Feasibility of a New Application of Noninvasive Brain Computer Interface (BCI): A Case Study of Training for Recovery of Volitional Motor Control after Stroke." *Journal of Neurologic Physical Therapy : JNPT* 33 (4): 203–11.

Darvas, F, D Pantazis, E Kucukaltun-Yildirim, and R M Leahy. 2004. "Mapping Human Brain Function with MEG and EEG: Methods and Validation." *NeuroImage* 23 Suppl 1 (January): S289–99.

Darvas, F, R Scherer, J G Ojemann, R P Rao, K J Miller, and L B Sorensen. 2010. "High Gamma Mapping Using EEG." *NeuroImage* 49 (1). Elsevier Inc.: 930–38.

Darvas, Felix, Rajesh P N Rao, and Micheal Murias. 2013. "Localized High Gamma Motor Oscillations Respond to Perceived Biologic Motion." *Journal of Clinical Neurophysiology : Official Publication of the American Electroencephalographic Society* 30 (3): 299–307.

De Lange, Floris P, Ole Jensen, Markus Bauer, Ivan Toni, and Floris P de Lange. 2008. "Interactions between Posterior Gamma and Frontal Alpha/beta Oscillations during Imagined Actions." *Frontiers in Human Neuroscience* 2 (August).

di Pellegrino, G, and SP Wise. 1991. "A Neurophysiological Comparison of Three Distinct Regions of the Primate Frontal Lobe." *Brain : A Journal of Neurology* 114 (2): 951–78.

Duun-Henriksen, Jonas, Troels Wesenberg Kjaer, David Looney, Mary Doreen Atkins, Jens Ahm Sørensen, Martin Rose, Danilo P Mandic, Rasmus Elsborg Madsen, and Claus Bogh Juhl. 2015. "EEG Signal Quality of a Subcutaneous Recording System Compared to Standard Surface Electrodes." *Journal of Sensors* 2015: 1–9.

Friedrich, Elisabeth V C, Reinhold Scherer, and Christa Neuper. 2012. "The Effect of Distinct Mental Strategies on Classification Performance for Brain-Computer Interfaces." *International Journal of Psychophysiology : Official Journal of the International Organization of Psychophysiology* 84 (1). Elsevier B.V.: 86–94.

Georgopoulos, a P, J F Kalaska, R Caminiti, and J T Massey. 1982. "On the Relations between the Direction of Two-Dimensional Arm Movements and Cell Discharge in Primate Motor Cortex." *The Journal of Neuroscience : The Official Journal of the Society for Neuroscience* 2 (11): 1527–37.

Georgopoulos, Apostolos P. 1989. "Cognitive Spatial-Motor Processes. 3. Motor Cortical Prediction of Movement Direction during an Instructed Delay Period." *Experimental Brain Research* 75 (1): 183.

Ghosh, S, and R Gattera. 1995. "A Comparison of the Ipsilateral Cortical Projections to the Dorsal and Ventral Subdivisions of the Macaque Premotor Cortex." *Somatosens Mot Res* 12 (3-4): 359–78.

Haase, A, J Frahm, D Matthaei, W Haenicke, and KD Merboldt. 1986. "FLASH Imaging: Rapid NMR Imaging Using Low Flip Angles Pulses." *J Magn Reson* 67: 258–66.

Hatsopoulos, Nicholas, Jignesh Joshi, and John G O'Leary. 2004. "Decoding Continuous and Discrete Motor Behaviors Using Motor and Premotor Cortical Ensembles." *Journal of Neurophysiology* 92 (2): 1165–74.

Hermes, Dora, Kai J Miller, Mariska J Vansteensel, Erik J Aarnoutse, Frans S S Leijten, and Nick F Ramsey. 2012. "Neurophysiologic Correlates of fMRI in Human Motor Cortex." *Human Brain Mapping* 33 (7): 1689–99.

Hinkley, Leighton B N, Srikantan S Nagarajan, Sarang S Dalal, Adrian G Guggisberg, and Elizabeth a Disbrow. 2011. "Cortical Temporal Dynamics of Visually Guided Behavior." *Cerebral Cortex (New York, N.Y. : 1991)* 21 (3): 519–29.

Huang, N. E. Z., S. R. Shen, M. C. Long, H. H. Wu, Q. Shih, N.-C. Zheng, C. C. Yen, H. H. Tung, and Liu. 1998. "The Empirical Mode Decomposition and the Hilbert Spectrum for Nonlinear and Non-Stationary Time Series Analysis." In *Proceedings of the Royal Society A, London*, 903–95.

Jerbi, Karim, Samson Freyermuth, Sarang Dalal, Philippe Kahane, Olivier Bertrand, Alain Berthoz, and Jean-Philippe Lachaux. 2009. "Saccade Related Gamma-Band Activity in Intracerebral EEG: Dissociating Neural from Ocular Muscle Activity." *Brain Topography* 22 (1): 18–23.

Kakei, S, D S Hoffman, and P L Strick. 2001. "Direction of Action Is Represented in the Ventral Premotor Cortex." *Nature Neuroscience* 4 (10): 1020–25.

Kalaska, J F, R Caminiti, and AP Georgopoulos. 1983. "Cortical Mechanisms Related to the Direction of Two-Dimensional Arm Movements- Relations in Parietal Area 5 and Comparison with Motor cortex_Exp Brain Res.pdf." *Experimental Brain Research* 51: 247–60.

Leuthardt, Eric C, Kai J Miller, Gerwin Schalk, Rajesh P N Rao, and Jeffrey G Ojemann. 2006. "Electrocorticography-Based Brain Computer Interface--the Seattle Experience." *IEEE Transactions on Neural Systems and Rehabilitation Engineering : A Publication of the IEEE Engineering in Medicine and Biology Society* 14 (2): 194–98.

Logothetis, N K, J Pauls, M Augath, T Trinath, and a Oeltermann. 2001. "Neurophysiological Investigation of the Basis of the fMRI Signal." *Nature* 412 (6843): 150–57.

M. Yutchman, A. Suzuki B.D. Van Veen W. van Drongelen. 1997. "Location of Brain Electrical Activity via Linearly Constrained Minimum Variance Spatial Filtering." *IEEE Trans Biomed Eng* 44: 867–80.

Manning, Jeremy R, Joshua Jacobs, Itzhak Fried, and Michael J Kahana. 2009. "Broadband Shifts in Local Field Potential Power Spectra Are Correlated with Single-Neuron Spiking in Humans." *The Journal of Neuroscience : The Official Journal of the Society for Neuroscience* 29 (43): 13613–20.

Martz, Gabriel U., Christina Hucek, and Mark Quigg. 2009. "Sixty Day Continuous Use of Subdermal Wire Electrodes for Eeg Monitoring during Treatment of Status Epilepticus." *Neurocritical Care* 11 (2): 223–27.

Matelli, M, P Govoni, C Galletti, D.F. Kutz, and Giuseppe Luppino. 1998. "Superior Area 6 Afferents from the Superior Parietal Lobule in the Macaque Monkey." *Journal of Comparative Neurology* 403 (3): 327–52.

McFarland, Dennis J, LA Miner, Theresa M Vaughan, and JR Wolpaw. 2000. "Mu and Beta Rhythm Topographies during Motor Imagery and Actual Movements." *Brain Topogr* 12 (3): 177–86.

Miller, K J, S Zanos, E E Fetz, M den Nijs, and J G Ojemann. 2009. "Decoupling the Cortical Power Spectrum Reveals Real-Time Representation of Individual Finger Movements in Humans." *The Journal of Neuroscience : The Official Journal of the Society for Neuroscience* 29 (10): 3132–37.

Miller, Kai J, Eric C Leuthardt, Gerwin Schalk, Rajesh P N Rao, Nicholas R Anderson, Daniel W Moran, John W Miller, and Jeffrey G Ojemann. 2007. "Spectral Changes in Cortical Surface

Potentials during Motor Movement." *The Journal of Neuroscience : The Official Journal of the Society for Neuroscience* 27 (9): 2424–32.

Miller, Kai J, Kurt E Weaver, and Jeffrey G Ojemann. 2009. "Direct Electrophysiological Measurement of Human Default Network Areas." *Proceedings of the National Academy of Sciences of the United States of America* 106 (29): 12174–77.

Miller, Kai, Gerwin Schalk, Eberhard E Fetz, Marcel den Nijs, Jeffrey G Ojemann, and Rajesh P N Rao. 2010. "Cortical Activity during Motor Execution, Motor Imagery, and Imagery-Based Online Feedback." *Proceedings of the National Academy of Sciences of the United States of America* 107 (15): 7113.

Mukamel, Roy, Hagar Gelbard, Amos Arieli, Uri Hasson, Itzhak Fried, and Rafael Malach. 2005. "Coupling between Neuronal Firing, Field Potentials, and FMRI in Human Auditory Cortex." *Science (New York, N.Y.)* 309 (5736): 951–54.

Murakami, Shingo, and Yoshio Okada. 2006. "Contributions of Principal Neocortical Neurons to Magnetoencephalography and Electroencephalography Signals." *The Journal of Physiology* 575 (3): 925–36.

Neuper, C, and G Pfurtscheller. 2001. "Event-Related Dynamics of Cortical Rhythms: Frequency-Specific Features and Functional Correlates." *International Journal of Psychophysiology : Official Journal of the International Organization of Psychophysiology* 43 (1): 41–58.

Neuper, Christa, Reinhold Scherer, Miriam Reiner, and Gert Pfurtscheller. 2005. "Imagery of Motor Actions: Differential Effects of Kinesthetic and Visual-Motor Mode of Imagery in Single-Trial EEG." *Brain Research. Cognitive Brain Research* 25 (3): 668–77.

Niedermeyer, Ernst, and Fernando Lopes da Silva. 2004. *Electroencephalography: Basic Principles, Clinical Applications, and Related Fields*.

Niessing, Jörn, Boris Ebisch, Kerstin E Schmidt, Michael Niessing, Wolf Singer, and Ralf a W Galuske. 2005. "Hemodynamic Signals Correlate Tightly with Synchronized Gamma Oscillations." *Science (New York, N.Y.)* 309 (5736): 948–51.

Nunez, Paul L., and Richard B. Silberstein. 2000. "On the Relationship of Synaptic Activity to Macroscopic Measurements: Does Co-Registration of EEG with fMRI Make Sense?" *Brain Topography* 13 (2). Kluwer Academic Publishers-Plenum Publishers: 79–96.

Ogawa, S, TM Lee, AS Nayak, and P Glynn. 1990. "Oxygenation-Sensitive Contrast in Magnetic Resonance Image of Rodent Brain at High Magnetic Fields." *Magnetic Resonance Imaging* 12 (1): 68–78.

Olson, Jared D, Jeremiah D Wander, and Felix Darvas. n.d. "Characterization of Beta and High Gamma Brain Signals in Subdermal Electroencephalography Recordings." *Unpub*.

Olson, Jared D., Jeremiah D. Wander, Lise Johnson, Devapratim Sarma, Kurt Weaver, Edward J. Novotny, Jeffrey G. Ojemann, and Felix Darvas. 2015. "Comparison of Subdural and Subgaleal Recordings of Cortical High-Gamma Activity in Humans." *Clinical Neurophysiology*. International Federation of Clinical Neurophysiology.

Ozerdem, A, B Guntekin, Mi Atagun, and E Basar. 2012. "Brain Oscillations in Bipolar Disorder

in Search of New Biomarkers." *Clin Neurophysiol* 62: 207–21.

Pantazis, Dimitrios, Thomas E Nichols, Sylvain Baillet, and Richard M Leahy. 2005. "A Comparison of Random Field Theory and Permutation Methods for the Statistical Analysis of MEG Data." *NeuroImage* 25 (2): 383–94.

Penfield, W, and T Rasmussen. 1950. "The Cerebral Cortex ofMan; a Clinical Study of Localization of Function." *Macmillan Co., New York. Phillips*, 248.

Pfurtscheller, G, and F H Lopes da Silva. 1999. "Event-Related EEG/MEG Synchronization and Desynchronization: Basic Principles." *Clinical Neurophysiology : Official Journal of the International Federation of Clinical Neurophysiology* 110 (11): 1842–57.

Pfurtscheller, G, and C Neuper. 2006. "Future Prospects of ERD/ERS in the Context of Brain-Computer Interface (BCI) Developments." *Prog Brain Res* 159: 433–47.

Pfurtscheller, G, C Neuper, G R Müller, B Obermaier, G Krausz, a Schlögl, R Scherer, et al. 2003. "Graz-BCI: State of the Art and Clinical Applications." *IEEE Transactions on Neural Systems and Rehabilitation Engineering : A Publication of the IEEE Engineering in Medicine and Biology Society* 11 (2): 177–80.

Prasad, Girijesh, Pawel Herman, Damien Coyle, Suzanne McDonough, and Jacqueline Crosbie. 2010. "Applying a Brain-Computer Interface to Support Motor Imagery Practice in People with Stroke for Upper Limb Recovery: A Feasibility Study." *Journal of Neuroengineering and Rehabilitation* 7 (1). BioMed Central Ltd: 60.

Ramos-Murguialday, Ander, Doris Broetz, Massimiliano Rea, Leonhard Läer, Ozge Yilmaz, Fabricio L Brasil, Giulia Liberati, et al. 2013. "Brain-Machine Interface in Chronic Stroke Rehabilitation: A Controlled Study." *Annals of Neurology* 74 (1): 100–108.

Rao, Rajesh P N. 2013. *Brain-Computer Interfacing: An Introduction*. Cambridge, UK: Cambridge University Press.

Reid, Andrew T, and Alan C Evans. 2013. "Structural Networks in Alzheimer's Disease." *European Neuropsychopharmacology : The Journal of the European College of Neuropsychopharmacology* 23 (1). Elsevier: 63–77.

Reva, N V, and L I Aftanas. 2004. "The Coincidence between Late Non-Phase-Locked Gamma Synchronization Response and Saccadic Eye Movements." *International Journal of Psychophysiology : Official Journal of the International Organization of Psychophysiology* 51 (3): 215–22.

Rombouts, S a, F Barkhof, F G Hoogenraad, M Sprenger, J Valk, and P Scheltens. 1997. "Test-Retest Analysis with Functional MR of the Activated Area in the Human Visual Cortex." *AJNR. American Journal of Neuroradiology* 18 (7): 1317–22.

Russo, G S, and C J Bruce. 1994. "Frontal Eye Field Activity Preceding Aurally Guided Saccades." *Journal of Neurophysiology* 71 (3): 1250–53.

Saad, Ziad S, Kristina M Ropella, Edgar a DeYoe, and Peter a Bandettini. 2003. "The Spatial Extent of the BOLD Response." *NeuroImage* 19 (1): 132–44.

Schwartz, a B, R E Kettner, and a P Georgopoulos. 1988. "Primate Motor Cortex and Free Arm

Movements to Visual Targets in Three-Dimensional Space. I. Relations between Single Cell Discharge and Direction of Movement." *J.Neurosci.* 8 (August): 2913–27.

Sellers, Eric W., Dean J. Krusienski, Dennis J. McFarland, Theresa M. Vaughan, and Jonathan R. Wolpaw. 2006. "A P300 Event-Related Potential Brain-Computer Interface (BCI): The Effects of Matrix Size and Inter Stimulus Interval on Performance." *Biological Psychology* 73 (3): 242–52.

Shen, L, and G E Alexander. 1997. "Preferential Representation of Instructed Target Location versus Limb Trajectory in Dorsal Premotor Area." *Journal of Neurophysiology* 77 (3): 1195–1212.

Shima, Keisetsu, Jun Tanji, Terra D Barnes, Jian-bin Mao, Dan Hu, Yasuo Kubota, Anna a Dreyer, Catherine Stamoulis, Emery N Brown, and Ann M Graybiel. 2000. "Neuronal Activity in the Supplementary and Presupplementary Motor Areas for Temporal Organization of Multiple Movements Neuronal Activity in the Supplementary and Presupplementary Motor Areas for Temporal Organization of Multiple Movements." *Journal of Neurophysiology* 84 (4): 2148–60.

Smith, MM, KE Weaver, T Grabowski, RPN Rao, and F Darvas. 2014. "Non-Invasive Detection of High Gamma Band Activity during Motor Imagery." *Frontiers in Human Neuroscience*, 8:817.

Subramaniyam, Narayan Puthanmadam, Katrina Wendel, Atte Joutsen, and Jari Hyttinen. 2011. "Investigating the Measurement Capability of Densely-Distributed Subdermal EEG Electrodes." *2011 8th International Symposium on Noninvasive Functional Source Imaging of the Brain and Heart and the 2011 8th International Conference on Bioelectromagnetism, NFSI and ICBEM 2011* 0 (3): 109–13..

Tadel, François, Sylvain Baillet, John C Mosher, Dimitrios Pantazis, and Richard M Leahy. 2011. "Brainstorm: A User-Friendly Application for MEG/EEG Analysis." *Computational Intelligence and Neuroscience* 2011 (January): 879716.

Tanji, J, and E Hoshi. 2008. "Role of the Lateral Prefrontal Cortex in Executive Behavioral Control." *Physiological Reviews* 88 (140): 37–57. doi:10.1152/physrev.00014.2007.

Trujillo, Logan T, Mary a Peterson, Alfred W Kaszniak, and John J B Allen. 2005. "EEG Phase Synchrony Differences across Visual Perception Conditions May Depend on Recording and Analysis Methods." *Clinical Neurophysiology : Official Journal of the International Federation of Clinical Neurophysiology* 116 (1): 172–89.

Vecchio, F, C Babiloni, R Lizio, FV Fallani, K Blinowska, G Verrienti, G Frisoni, and PM Rossini. 2013. "Resting State Cortical EEG Rhythms in Alzheimer's Disease: Towards EEG Markers for Clinical Applications. A Review." *Clin Neurophysiol* 62: 223–36.

Weinrich, M, and S P Wise. 1982. "The Premotor Cortex of the Monkey." *The Journal of Neuroscience : The Official Journal of the Society for Neuroscience* 2 (9): 1329–45.

Wendel, Katrina, Juho Väisänen, Gunnar Seemann, Jari Hyttinen, and Jaakko Malmivuo. 2010. "The Influence of Age and Skull Conductivity on Surface and Subdermal Bipolar EEG Leads." *Computational Intelligence and Neuroscience* 2010.

Whittingstall, Kevin, and Nikos K Logothetis. 2009. "Frequency-Band Coupling in Surface EEG

Reflects Spiking Activity in Monkey Visual Cortex." *Neuron* 64 (2). Elsevier Ltd: 281–89.

Wolpaw, Jonathan R, Niels Birbaumer, Dennis J McFarland, Gert Pfurtscheller, and Theresa M Vaughan. 2002. "Brain-Computer Interfaces for Communication and Control." *Clinical Neurophysiology : Official Journal of the International Federation of Clinical Neurophysiology* 113 (6): 767–91.

Yener, GG, and E Bajar. 2012. "Brain Oscillations as Biomarkers in Neuropsychiatric Disorders: Following an Interactive Panel Discussion and Synopsis." *Clin Neurophysiol* 62: 237–57.

Yener, GG, and E Basar. 2012. "Biomarkers in Alzheimer's Disease with a Special Emphasis on Event-Related Oscillatory Responses." *Clin Neurophysiol* 62: 325–60.

Young, G Bryan, John R Ives, Martin G Chapman, and Seyed M Mirsattari. 2006. "A Comparison of Subdermal Wire Electrodes with Collodion-Applied Disk Electrodes in Long-Term EEG Recordings in ICU." *Clinical Neurophysiology : Official Journal of the International Federation of Clinical Neurophysiology* 117 (6): 1376–79.

Yuan, Han, Tao Liu, Rebecca Szarkowski, Cristina Rios, James Ashe, and Bin He. 2010. "Negative Covariation between Task-Related Responses in Alpha/beta-Band Activity and BOLD in Human Sensorimotor Cortex: An EEG and fMRI Study of Motor Imagery and Movements." *NeuroImage* 49 (3). Elsevier Inc.: 2596–2606.

Yuval-Greenberg, Shlomit, Orr Tomer, Alon S Keren, Israel Nelken, and Leon Y Deouell. 2008. "Transient Induced Gamma-Band Response in EEG as a Manifestation of Miniature Saccades." *Neuron* 58 (3): 429–41. doi:10.1016/j.neuron.2008.03.027.

VITA

Melissa Smith was born in Albuquerque, NM in 1982. She completed her Bachelor of Science degree in Cellular Biology at Western Washington University in 2005. After graduating college she joined a neuroscience lab at Seattle Children's Research Institute, where she was influenced to pursue graduate school in neuroscience. After enrolling in the Graduate Program for Neuroscience at the University of Washington Melissa joined the lab of Dr. Rajesh Rao in 2011.